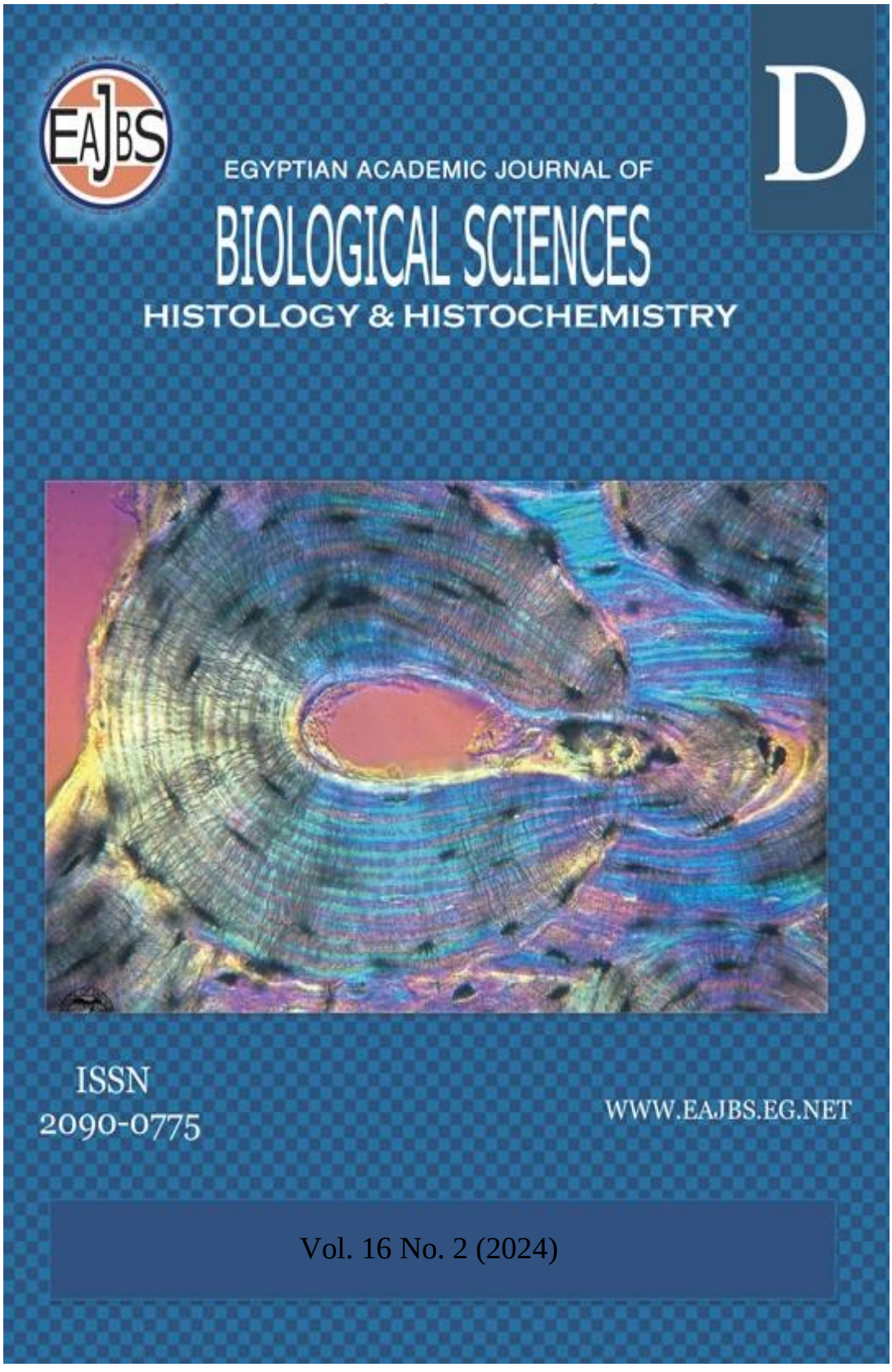

Citation: Egypt. *Acad. J. Biolog. Sci. (D-Histology and histochemistry) Vol.16(2) pp27-55(2024)*
DOI: 10.21608/EAJBSD.2024.372658

Egypt. Acad. J. Biolog. Sci., 16(2): 27-55 (2024)

Egyptian Academic Journal of Biological Sciences
D. Histology & Histochemistry
ISSN 2090 – 0775
http://eajbsd.journals.ekb.eg

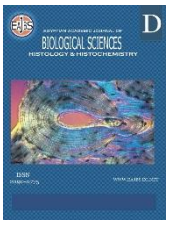

Could Peri-natal Exposure to Red Bull Induced Damage in the Heart and Lung in Rat Offsprings: Histological, Ultra-structural, and Immunohistochemical Study?

Hala M. Hassanin and Sally S. Anwer
Department of Human Anatomy and Embryology, Faculty of Medicine, Assiut University, Assiut, Egypt.
*** E-mail** : halahasenien@aun.edu.eg ; Sallysayed@aun.edu.eg

ARTICLE INFO
Article History
Received:7/6/2024
Accepted:8/ 8/2024
Available:12/8/2024

***Keywords*:**
Red Bull, heart, lung.

ABSTRACT

Introduction: Energy drinks (ED) are utilized all over the world. The components of (ED) have desired effects such as increasing energy but they produce undesired effects on health. **Aim of the work**: to assess the effects of consumption of Red Bull during pregnancy on the structure of the heart and lungs. **Methodology:** this study was conducted on 30 grown-up female rats divided into three groups (10 in each group). Control group, Low dose treated group (received Red Bull 2.5 ml/kg body weight by oral gavage from the first day of pregnancy till the 21st day after birth, and High dose treated group (got Red Bull 5 ml/kg body weight orally via oral gavage from the beginning of pregnancy till the 21st day after birth). The hearts and lungs of newborn and 21st-day-old offspring were extracted and processed. **Results:** Red Bull consumption induced destructive changes in the heart and lungs as loss of regular arrangement of myofibrils, dilation of congested blood vessels and infiltration of peri-vascular cells and areas of degeneration and lysis. In the lung, there was distortion in lung architecture, an increase in the thickness of inter-alveolar septum, and abnormality in pneumocytes type 1 and 2.
Conclusion: The consumption of Red Bull in the peri-natal period, especially in high doses, has marked destructive effects on the heart and lungs.

INTRODUCTION

Energy drinks (ED) are now well known and excessively utilized all over the world, especially by young adults as they improve mental and physical performance (Vercammen *et al.,* 2019). Various energy drink varieties, such as Power Horse, Tiger and Red Bull are available in Egyptian markets, all of them contain caffeine, sucrose, B vitamins, ginseng, carbohydrates, taurine, minerals and water other herbal extracts (Higgins *et al.,* 2010).

Although the components of (ED) have desired effects such as increasing energy, rise in physical and mental activity, and mood elevation at the same time these components can produce undesired effects and have a bad impact on health (Geith, 2017), such as nephrotoxicity (Khayyat *et al.*, 2014), hematological abnormalities (Olaleru and Odeigah, 2015), inflammation in the liver and pancreas (Uwaifo, 2019). Furthermore, a marked increase in body weight and type II diabetes may result from its high sugar content (Adjene *et al.,* 2014). Most of the body organs and systems are affected by the consumption of energy drinks such as the brain, cardiovascular system, and skeletal system (Curran and Marczinski, 2017). There were studies supporting that; consumption of energy drinks is related to immune disorders and allergic reactions (Wee *et al.,* 2020).

The utilization of Energy drinks has markedly increased all over the world during the past few years. Public health problems appeared despite claims of being safe and beneficial (Kaur *et al.,* 2022).

Lipid peroxidation increased significantly in newborns exposed to the ED and Numerous organs, including the brain, kidney, and liver, showed a decline in antioxidant activity of the newborns, 21 and 35-day-old offspring. ED induced multiple alterations in the histological structure of hepatocytes, kidney, cerebral cortex, and cerebellum. Moreover, the loco-motor system was affected, ED augmented the locomotion and induced behavioral changes such as anxiety in mice newborns. pre-natal ED exposure causes oxidative stress, tissue damage, and altered behavior in the mice offspring (Al-Basher *et al.,* 2018).

Energy drinks consumption is related to bad cardiovascular effects. Energy drinks when taken in excess, are linked to several cardiac issues, such as palpitations, arrhythmia (ventricular and supra-ventricular ectopy) and atrial fibrillation. Coffee sharply increases blood pressure and stresses the cardiovascular system (Grasser *et al.,* 2015). Red Bull consumption induces alteration of pulmonary blood flow (Treml *et al.,* 2020).

As the consumption of energy drinks gained popularity all over the globe and because of their hazards to our health, there is a strong desire to perform trial research to assess and comprehend their impact on different body systems. There isn't much information at hand regarding the impact of peri-natal use of EDs on the cardiovascular system and lungs of offspring. The goal of the current study is to assess the effects of consumption of varying dosages (high and low) of Red Bull during pregnancy on the heart and lungs of newborn and 21-day-old offspring albino rats.

MATERIALS AND METHODS

Chemicals:

The Red Bull has 400 mg of taurine, 32 mg of caffeine, 240 mg of gluconolactone, 20 mg of inositol, 8 mg of niacin, 11.3 g of sucrose and glucose, 2.4 mg of pantothenic acid, vitamins B2/B6/B12, citric acid, and flavourings, colours per 100 millilitres, is what we used. It was obtained from the local Egyptian market. The product is offered in 250 ml cans.

Animals:

The study was conducted on 30 adult female albino rats aged three months, weighed (180-200) gm each and obtained from Animal House, Faculty of Medicine, Assiut University. The rats were kept in a clean ventilated cage with a 12/12-hour cycle of light and dark and optimal temperature of 23±2ºC, humidity (60±10%), Water and food were added continuously. Prior to the experiment's start the animals were kept for two weeks in the animal house for acclimatization.

Experimental Design:

The thirty adult female rats were kept with adult male rats (three females for one male) in an amazing cage for twelve hours, then, a vaginal plug was observed, and the day it appeared was regarded as the start of the pregnancy. From the first day of pregnancy, the female rats were split up at random into three groups (10 female rats in each group).

Group I: (**Control group**) rats in this group obtained purified water daily from the first day of pregnancy to the 21st day following delivery (end of the experiment) by oral gavage. Then the newborn and the 21-day-old offspring were sacrificed and their hearts and lungs were extracted, processed, and examined to measure the basic parameters.

Group II: (Low dose Red Bull treated group) Female rats in this group received Red Bull in a dose of 2.5 ml/kg body weight was administered by oral gavage from the first day of pregnancy to the 21st day after delivery (end of the experiment).

Group III: (High dose Red Bull treated group) Female rats in this group were given Red Bull in a dose of 5 ml/kg body weight was administered by oral gavage from the first day of pregnancy to the 21st day after delivery. These doses (high and

low) of Red Bull were chosen in accordance with (Al-Basher *et al.*, 2018).

The offsprings (newborn and 21st-day offsprings) of female rats from all groups were sacrificed after anaesthesia by pentobarbital (50 mg/kg), their chest walls were opened, and immediate perfusion was done by intra-cardiac neutralized buffered formalin was injected into the left ventricle until output from the right atrium appeared clear. After that, the hearts and lungs were extracted and prepared for morphometric, ultra-structural, immunohistochemical, and light microscopic investigations.

Light Microscopic Study:

The specimens of heart and lung were extracted from the offspring thoracic cavity, divided into smaller parts, and fixed for 24 to 48 hours in 10% formalin based on how big the samples were. Dehydration of specimens was performed after fixation by immersing them in ascending grades of ethyl alcohol. After that, the specimens were cleared, poured in paraffin wax, and cut into serial sagittal sections 5-7-micron thickness and Hematoxylin and Eosin staining used to illustrate the overall histological structure (Bancroft and Layton, 2019).

Electron Microscopic Study:

The specimens of the ultra-structural study were cut into small particles of about 1x1 ml and immediately fixed in cold 2.5% glutaraldehyde for 24 hours. After fixation, the samples were cleaned in phosphate buffer (pH 7.4) in four washes (each wash takes 20 minutes), exposed to 1% osmium tetra-oxide for one hour, and another four washes were performed in phosphate buffer (each wash takes 20 minutes), embedded in a mixture of epon araldite and dehydrated in ascending grades of ethyl alcohol. The specimens for semithin sections were cut in 0.5-micron thickness by (Deerfield, IL, USA), ultra-microtome and stained by toluidine blue, those for ultra-thin sections cut in 0.1-micron thickness, stained by uranyl acetate and lead acetate, and mounted on copper grids and photographed with a transmission electron microscope (TEM, Joel- JEM- 100 CXII; Joel, Tokyo, Japan) in Assiut University, electron microscopic unit (Woods and Stirling, 2019).

Immunohistochemical Study:

For the immune histochemical technique, the specimens were cut at 4 µm thickness and placed on positive-charged slides. Deparaffinization is performed by putting the sections in xylene. Then rehydration of sections is done through an ethanol series followed by phosphate-buffered saline (PBS) washing. Deactivation of the endogenous peroxide is done by using 10% hydrogen peroxide for ten minutes in phosphate-buffered saline. Then the incubation of sections with an anti-INOS polyclonal antibody (rabbit anti-rats INOS, M-19/Sc 650, Santa Cruz Biotechnology, Santa Cruz, CA, USA) diluted 1:100 was performed. Another three washes with phosphate-buffered saline (five minutes for each slide) after which the sections were incubated for 30 minutes with a biotinylated secondary antibody and followed by the streptavidin-peroxidase complex for 10 minutes at room temperature. Then the solution of diaminobenzidine (DAB) at 0.05% was added for visualization antigen-antibody reaction. Mayer's Hematoxylin was used to counterstain the sections. Then all sections were dehydrated and mounted, examined, and photographed at the Anatomy Department, Faculty of Medicine, Assiut University (Al Drees *et al.*, 2017).

Morphometric and Statistical Studies:

The inter-alveolar septum's thickness was measured at ten different non-overlapping fields from ten different specimens in each group at x 400 magnification using a computerized image analyzer system (Leica Q 500 MCO; Leica, Wetzlar, Germany) connected to a camera connected to a Leica universal microscope in Anatomy Department, Faculty of Medicine, Assiut University.

Statistical Analysis:

The SPSS software, version 26, was used to conduct the statistical analysis (SPSS Inc., Chicago, IL, USA). ANOVA, or one-way analysis of variance, was

utilized to elucidate the differences between the three groups. The data was shown as mean +/- standard deviation (SD), and statistical significance was defined as P-values of 0.05 or less (Connelly, 2021).

RESULTS

1. Histological Results:

A. Newborn Rats:

1. Heart:

1.1. Histopathological Alterations:

Light microscopic examination of control group sections stained with hematoxylin and eosin of cardiac muscle revealed the myofibers regularly arranged with their characteristic branching pattern, oval vesicular nuclei in the centre, and acidophilic sarcoplasm. In connective tissue spaces flattened fibroblast and blood vessels were noticed as illustrated in (Fig. 1a). However, in the low dose group the myofibers disorganized, some nuclei appeared degenerated, other nuclei became small and pyknotic, and the sarcoplasm showed many vacuoles. Moreover, the blood vessels appeared dilated, congested, and ruptured in some regions with extravasation of red blood cells between the cardiomyocytes as demonstrated in (Fig. 1b & 1c). Regarding the group receiving a high dose, there was a complete loss of regular pattern arrangement of myofibers, marked vacuolization of sarcoplasm, and all nuclei deformed and degenerated. The connective tissue spaces are markedly wider as compared to the control group and blood vessels dilated and congested as illustrated in (Fig. 1d, e& 1f).

In semithin sections stained with toluidine blue, the control group exhibited normal parrel myofibers, central oval vesicular nuclei, and normal blood vessels in thin connective tissue space among the cardiomyocytes (Fig. 2a), while in low dose group, some of the nuclei lost its normal oval pattern and deformed, the sarcoplasm appeared vacuolated in some regions and some blood vessels appeared dilated and congested (Fig. 2b). Regarding the high dose group, the myofibers appeared thinner, most of nuclei lost its oval pattern and deformed, massive vacuolization of sarcoplasm was noticed as compared to control group. Moreover, the blood vessels exhibited marked dilation and congestion (Fig. 2c).

1.2. Ultra-Structural Changes:

Examination of electron micrographs of the control group exhibited cardiomyocytes with oval euchromatic nuclei and numerous intact mitochondria in the perinuclear region. The myofibers appeared intact with preserved striation as illustrated in (Fig 3a). In the low-dose group, the myofibers appeared intact with preserved striations, and nuclei looked euchromatic, slightly indented with prominent nucleolus but vacuolization of sarcoplasm was noticed (Fig. 3 b, c).

On the other hand, examination of the high dose group showed major destructive changes in the form of thinning and atrophy of myofibers, degeneration and lysis of other myofibers, nuclei markedly indented, the sarcoplasm rarified and vacuolated, the mitochondria destructed and red blood cell extravasation was noticed (Fig.3 d, 3e).

2. Lung:

2.1. Histopathological Alterations:

Light microscopic examination of sections stained with eosin and hematoxylin of the control lung demonstrated the typical lung architecture; alveoli, alveolar sac, alveolar duct, and bronchiole lined with normal stratified epithelium. The thin inter-alveolar septum is lined with type I flattened pneumocytes, type II cuboidal pneumocytes as well as blood vessels (Fig. 4a, 4b). In low dose group, the lung architecture was disturbed to some extent as some of the alveoli collapsed, the bronchiolar epithelium degenerated, the inter-alveolar septum showed apparent increase in thickness, and the blood vessels exhibited congestion **(**Fig. 4c). Regarding the high dose group, there was complete disorganization of lung architecture; some alveoli was collapsed, marked increase in thickness of inter-alveolar septum with monocellular infiltration, there was a clear, noticeable increase in blood vessel congealing and red blood cell extravasation **(**Fig. 4d).

Upon examining the newborn lung of the control group's semithin sections stained with toluidine blue revealed the normal alveolar lumen lined by type 1 flattened pneumocytes with a narrow cytoplasmic rim and type 2 pneumocytes with a large, rounded nucleus and cytoplasm that is vacuolated. Alveolar macrophage with its characteristic kidney-shaped nucleus and relatively thin inter-alveolar septum were apparent **(**Fig. 5a). In the low dose group, there was an apparent increase in thickness of inter-alveolar septum and increase in macrophage relative to the control group **(**Fig. 5b). Regarding the high dose group there was massive distortion of lung architecture, collapsed alveoli, extrusion of some cells in alveolar lumen, apparent increase in type 2 pneumocytes and macrophages. The inter-alveolar septum showed a marked obvious increase in thickness. There were widespread congested dilated blood capillaries **(**Fig. 5c& 5d).

2.2. Ultra-Structural Changes:

Examination of electron micrographs of the lung in the control group showed the alveoli lined by type 1&2 pneumocytes. Type 1 showed characteristics of flattened euchromatic nuclei and thin cytoplasmic rim. Type 2 exhibited big euchromatic nuclei, unique lamellar bodies, numerous intact mitochondria, characteristic alveolar border, and rough endoplasmic reticulum (Fig. 6a, 6b). On examination of the low-dose group, type 1 pneumocytes appeared normal while type 2 showed heterochromatic nuclei with clumps of chromatin, swollen mitochondria, and vacuolated lamellar bodies (Fig. 6c, 6d). Regarding the high dose group, there was marked disturbance in type 1&2 pneumocytes as type 1 pneumocytes exhibited shrunken heterochromatic nucleus while type 2 pneumocytes showed indented nucleus, vacuolated cytoplasm, and numerous lipid droplets (Fig. 6e).

B. 21 Days Old Rats:

1.Heart

1.1. Histopathological Alterations:

Examination of Hematoxylin and eosin-stained portions of the control group's heart showed normal branching, anastomosing cardiomyocytes with large oval central vesicular nuclei and acidophilic cytoplasm. Narrow connective tissue space between the cardiomyocytes, fibroblast, and blood capillaries was shown (Fig. 7a). In the low-dose group, examination of the heart revealed apoptotic and inflammatory changes in cardiomyocytes as some nuclei appeared small, deeply stained, vacuolated cytoplasm and the blood vessels seemed to be dilated, congested. Additionally, red blood cell extravasation between the cardiomyocytes and peri-vascular cellular infiltration was detected (Fig.7b & 7c). Examination of the high dose group revealed marked destructive changes in the heart as the cardiomyocytes showed complete disorganization and loss of the branching anastomosing pattern with areas of degeneration and lysis, nuclei appeared small, rounded, deeply stained and the cytoplasm appeared highly acidophilic in addition, the blood capillaries showed marked dilatation, congestion, peri-vascular cellular infiltration, and red blood cell extravasation between the cardiomyocytes. Finally, wide connective tissue space and an apparent increase in fibroblast were noticed (Fig. 7d, 7e&7 f).

Semithin sections of the control group’s heart stained with toluidine blue revealed the cardiomyocytes with their normal characteristic striations. The intercalated disc was well demarcated (Fig. 8a). In the low-dose group, some nuclei lost their normal oval appearance (deformed), the cytoplasm vacuolated, and the blood capillaries showed marked dilatation and congestion. Moreover, the striation and the intercalated disc are not well demarcated (Fig. 8b&8 c). Regarding the high dose group, marked destructive changes were detected as there was a complete loss of branching anastomosing pattern of cardiomyocytes, myofibers showed marked thinning and atrophy, and sarcoplasm showed extensive vacuolization. Moreover, the blood capillaries exhibited marked obvious congestion and dilation (Fig. 8d& 8e).

1.2. Ultra-Structural Changes:

Examination of electron micrographs of the heart in the control group revealed regularly arranged myofibers with their characteristic striation and numerous intact mitochondria between the myofibers (Fig. 9a& 9b). In the group receiving a low dose, obvious changes were noticed but the general parrel appearance of myofibers was preserved apart from thinning observed in some myofibers. nucleus appeared abnormally shaped heterochromatic, sarcoplasm vacuolated and the mitochondria destructed (Fig. 9c& 9d). Regarding the high dose group, massive destructive changes as the myofibers exhibited complete loss of its regular parrel appearance, and loss of demarcation of light and dark bands with areas of degeneration and lysis. Nuclei indented, sarcoplasm showed massive vacuolization and the mitochondria exhibited extensive destruction (Fig. 9e& f).

1.3. Immunohistochemical Reaction:

Examination of INOS immunohistochemically stained sections of the control group's heart exhibited minimal light brown positive immunostaining of cytoplasm (Fig. 10a). In low dose group, moderate positive immunostaining of cytoplasm was apparent (Fig. 10b). Regarding the high dose group, strong positive immunostaining of cytoplasm was noticed (Fig. 10c).

2.Lung:

2.1. Histopathological Alterations:

On examination of sections stained with hematoxylin and eosin, the control group's lung displayed patent alveoli, thin inter-alveolar septum lined by flattened type 1 pneumocytes and cuboidal type 2 pneumocytes. The bronchioles lined by normal stratified epithelium and the blood vessels were apparent (Fig. 11a). In low dose group, some changes were detected as compared to the control; there were collapsed alveoli, apparent thickening of the inter-alveolar septum, disorganized bronchiolar epithelium, dilated, clogged blood vessels and peri-vascular cellular infiltration with deposition of eosinophilic material in blood vessels (Fig. 11b). Examination of the high dose group revealed, complete loss of normal lung architecture; several alveoli appeared collapsed, an apparent marked increase in thickness of inter-alveolar septum, massive extensive red blood cell extravasation, marked cellular infiltration and destroyed bronchiolar epithelium (Fig. 11c).

An examination of toluidine blue stained semithin sections of 21 days lung control group, showed that type 1 pneumocyte-lined patent alveoli with their characteristic flattened nuclei enclosed by a narrow cytoplasmic rim and type 2 pneumocytes with a large, rounded nucleus and vacuolated cytoplasm. The alveolar macrophages with their characteristic kidney-shaped nucleus were also noticed (Fig. 12a). In the low dose group, some alveoli appeared collapsed with extrusion of pneumocytes into the alveolar lumen and dilated congested blood capillaries was obviously detected, in addition, there was apparent increase in number of pneumocytes type 2 (Fig. 12b&12 c). Regarding the high dose group, there was complete distortion and destruction of normal lung architecture, several alveoli collapsed with extrusion of cells into the alveolar lumen, dilated congested blood capillaries were spread all over the sections with extravasation of red blood cells, markedly thickened abnormal inter-alveolar septum was noticed and an apparent increase in pneumocytes type 2 also noticed (Fig. 12d).

2.2. Ultrastructural Changes:

The control group's lung electron micrographs revealed the alveolar space lined by type 1 flattened pneumocytes with a thin cytoplasmic rim and type 2 pneumocytes with its characteristic large round euchromatic nucleus. Alveolar macrophage with its characteristic kidney-shaped nucleus and blood vessels was apparent (Fig. 13a&13 b). In the low-dose group, the alveoli were lined by flattened type 1 pneumocytes and large type 2 pneumocytes which showed indented nucleus, vacuolated lamellar bodies and ballooned mitochondria (Fig. 13c&13d).

Regarding the high-dose group, type 1 pneumocyte were abnormally shaped with a heterochromatic shrunken nucleus, and type 2 pneumocytes showed indented nucleus, vacuolated lamellar bodies, and ballooned mitochondria. The characteristic micro alveolar border was apparent (Fig. 13e).

2.3. Immunohistochemical Reaction:

Examination of INOS sections stained with immunohistochemistry of the control group's lung revealed minimal light brown positive immunostaining (Fig. 14a). In low dose group, moderate positive immunostaining was detected (Fig. 14b). Regarding the high dose group, strong extensive positive immunostaining was noticed (Fig. 14c).

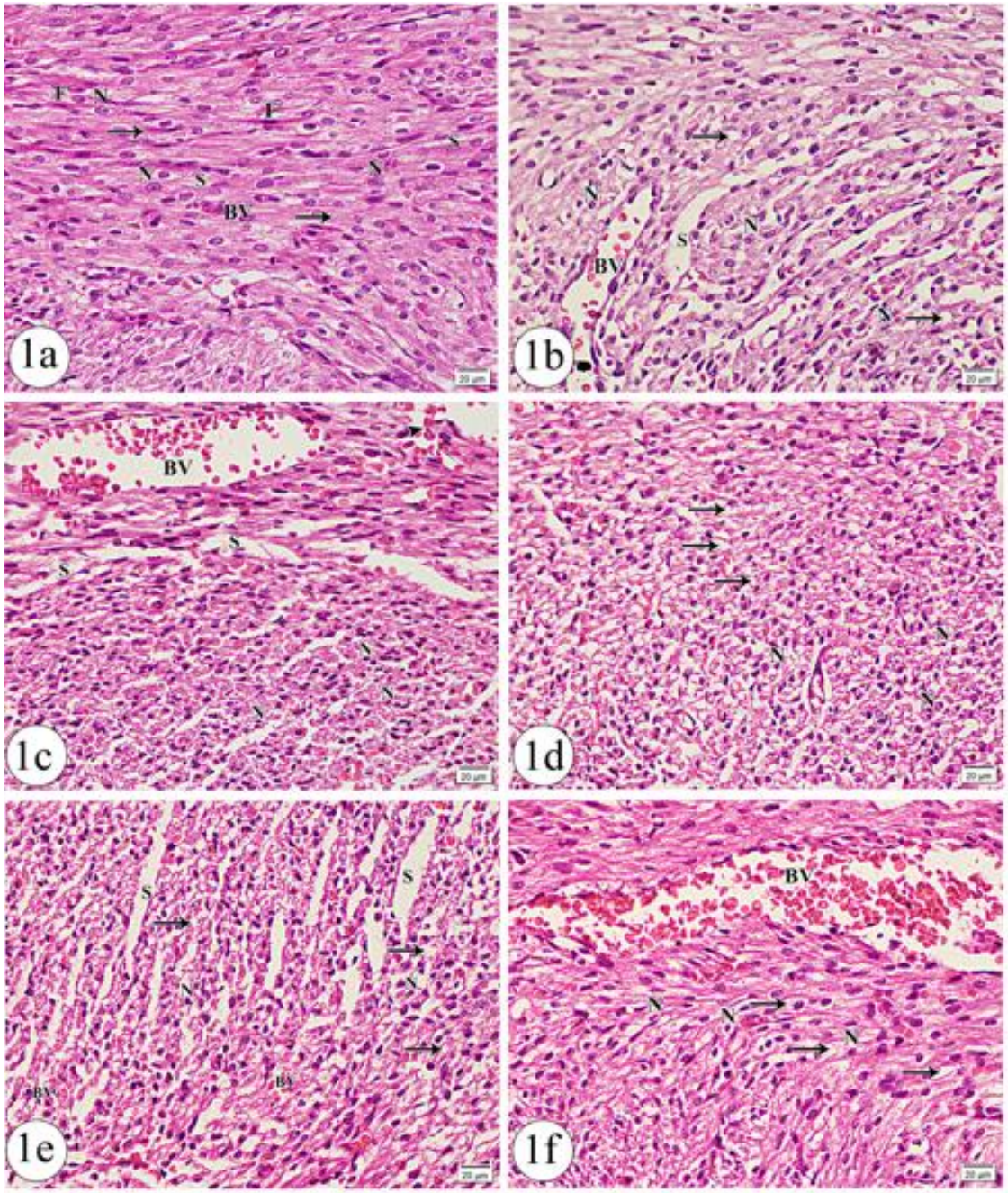

Fig.1 photomicrographs of longitudinal sections in the ventricular wall of newborn heart of control(1a) ,low dose (1b &1c) and high dose (1d, 1e & 1f) groups.[1a]:The cardiomyocytes showing normal branching pattern with large oval vesicular nuclei (N), acidophilic cytoplasm(arrow)and narrow connective tissue space in between the cardiomyocytes (S)containing flat nuclei of fibroblast (F) and blood capillaries(BV).[1b]:exhibiting vacuolated cytoplasm (arrow),some nuclei appeared degenerated (N)and marked widening of connective tissue space (S)with dilated congested blood capillaries(BV).[1c]**:**The cardiomyocytes showing loss of normal branching appearance with deformed small pyknotic nuclei(N) in some cells and marked widening of the space between the cardiac cells (S) with dilated ruptured blood capillaries and extravasation of red blood cells in between the cardiomyocytes (Arrow head).[1D]:showing complete loss of normal branching pattern with excessive marked vacuolization of cytoplasm(arrow) and deformed degenerated nuclei(N) in nearly all cells.[1E]: marked widening of space in between the cardiac cells(S), dilated congested blood capillaries(BV),vacuolated cytoplasm(arrow),small darkly stained nuclei(N)are observed.[1F]: massive dilatation and congestion in blood capillaries (BV),vacuolated cytoplasm(arrow)and small darkly stained nuclei(N).**(H&E × 400, Scale bar = 20 µm)**

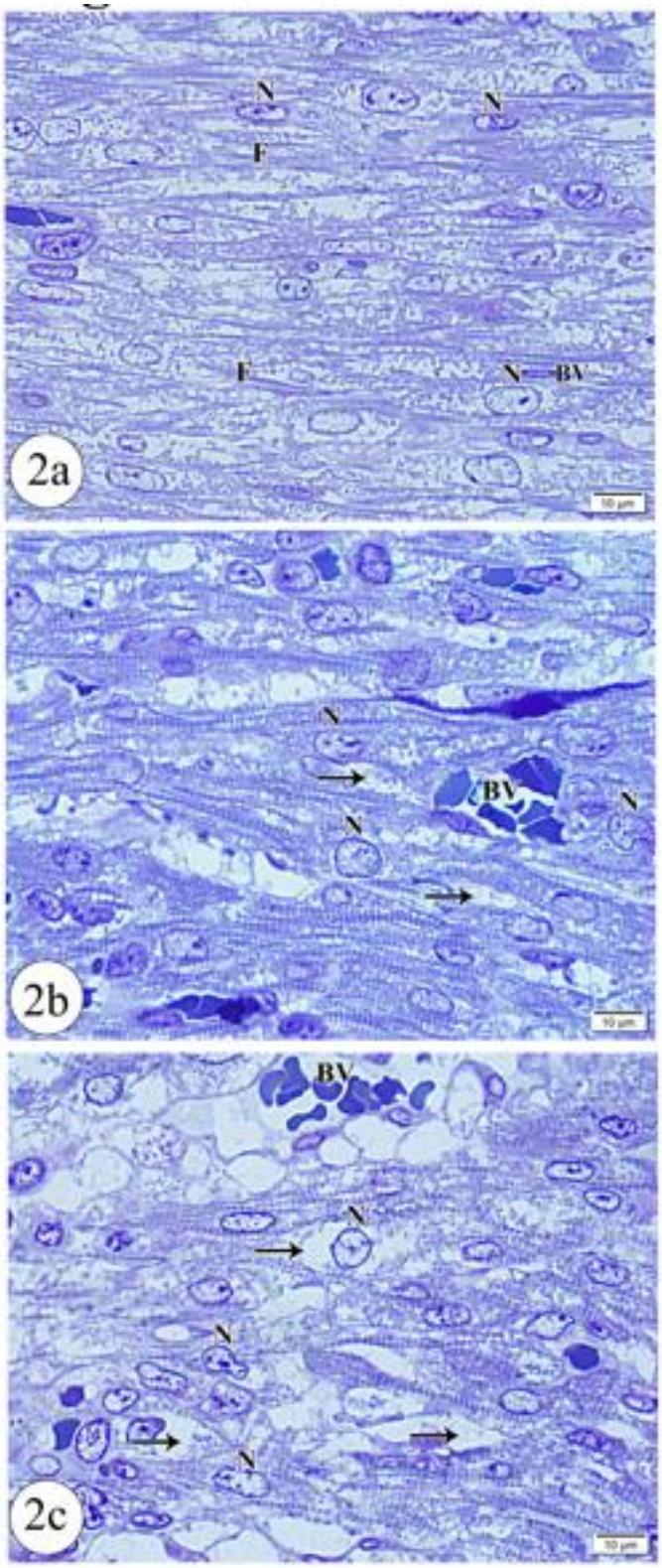

Fig.2 photomicrographs of semithin sections in newborn cardiomyocytes of control(2a), low dose(2b) and high dose(2c) groups. [2a]: showing the normal anastomosing parrell appearance of myofibrils(F), oval vesicular nuclei(N)and blood vessels (BV) in between the cardiac cells. [2b]: showing some deformed nuclei(N), multiple vacuoles(arrow) and dilated congested blood capillaries (BV). [2c]: showing loss of oval appearance in most of nuclei(N), extensive wide vacuolization in a major part of the section(arrow) and marked dilatation and congestion in blood capillaries (BV). **(Toluidine blue × 1000, Scale bar = 10 µm)**

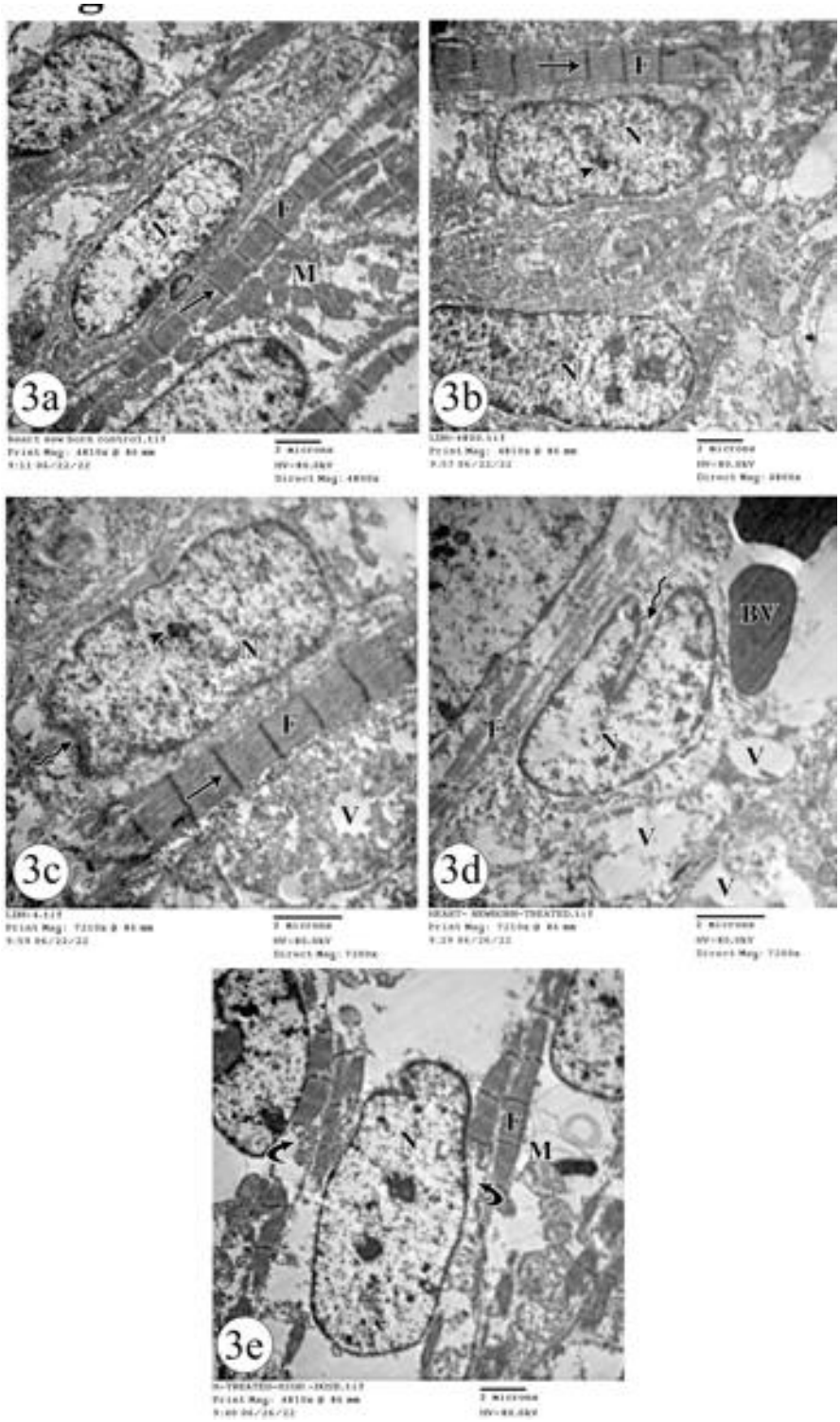

Fig.3 Electron micrographs of longitudinal sections in cardiomyocytes of new born rat in control(3a),low dose(3b,c) and high dose(3d,3e) groups.[3a]:showing normal oval euchromatic nuclei (N),large number of intact mitochondria in juxtanuclear region (M)and the myofibers appeared intact (F) with preserved striations (arrow).[3b,3C]:showing, oval euchromatic nuclei(N) with indentation in nuclear membrane (wavy arrow),prominent nucleolus (arrow head) ,intact myofibers (F) with preserved striation(Arrow) and many vacuoles are observed in sarcoplasm(V).[3d,3e]:showing deep indentation(wavy arrow) of nucleus (N), rarified vacuolated sarcoplasm(v) ,thinning and atrophy of myofibers with loss of striations (F).other myofibers showing areas of degeneration and lysis (curved arrow), extravasation of red blood cells (BV) and degenerated mitochondria(M) was noticed.
(TEM × 4800 In a, b, e TEM X 7200 in c, d Scale bar = 2 µm)

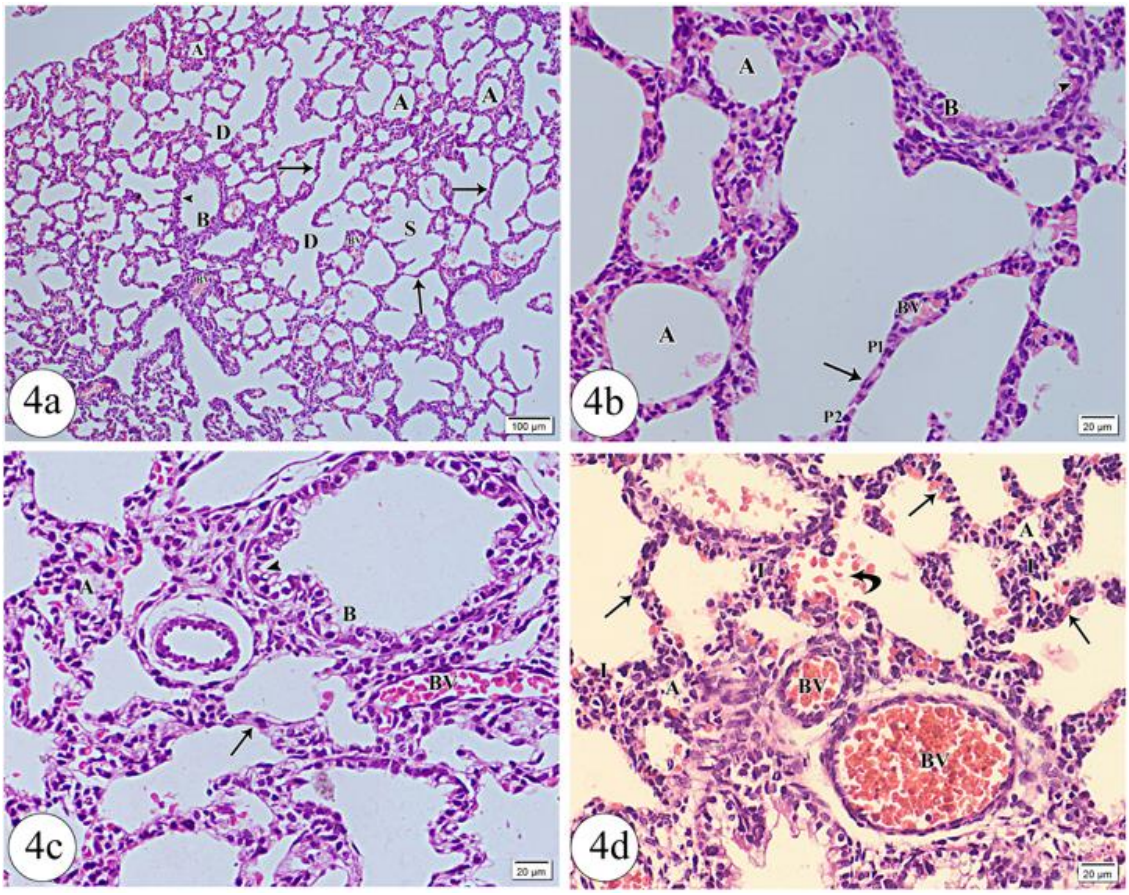

Fig.4 photomicrographs of longitudinal sections in new born lung from control (a& b),low dose (c) and high dose (d) groups.[4a,b]:showing the normal lung architecture including alveoli(A) ,alveolar sac (S),alveolar duct (D), bronchiole (B) with normal bronchiolar epithelium (arrow head) and blood vessels (BV).The thin interalveolar septum (arrow) with flattened pneumocyte type 1(P1) and cuboidal pneumocyte type 2 (P2) is noticed.[4c]: showing collapsed alveoli (A),apparent increase in thickness of interalveolar septum(arrow),bronchi (B) with degenerated bronchiolar epithelium(arrow head), and congested blood vessels (BV).[4d]:showing collapsed alveoli(A), obvious increased thickness of interalveolar septum(arrow) with cellular infiltration (I),massive congestion in blood vessels (BV)and extravasation of red blood cells(curved arrow).
(H&E × 100,4a) (H&E × 400, 4b,4c,4d Scale bar = 20 µm)

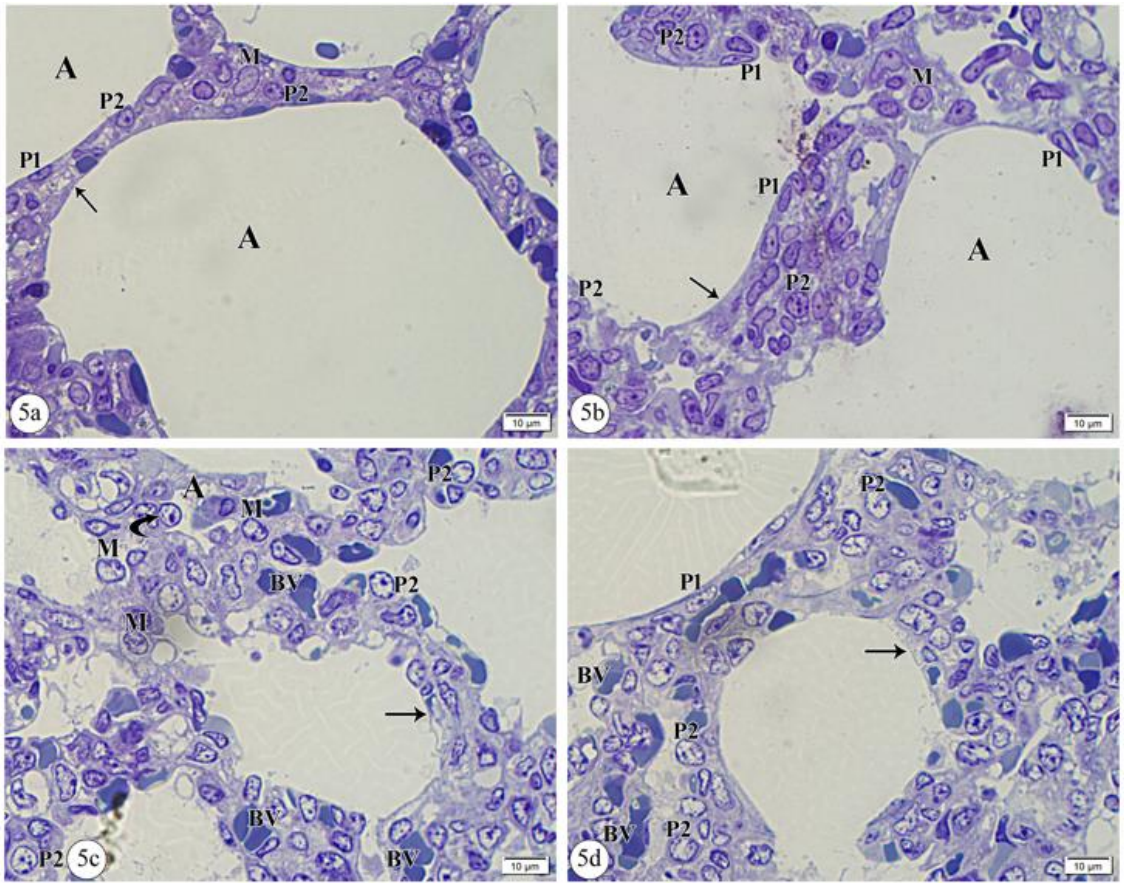

Fig.5 photomicrographs of semithin sections of new born lung of control(a),low dose(b) and high dose (c& d) groups.[5a]showing: the alveolar lumen(A),type 1 flattened pneumocytes (P1),type 2 pneumocytes (P2)with large round nucleus, alveolar macrophage(M) and relatively thin interalveolar septum(arrow) .[5b]showing: alveolar lumen (A),type 1 flattened pneumocytes (P1), type 2 pneumocytes (P2)with large round nucleus, alveolar macrophage(M) and relatively thick interalveolar septum (arrow).[5c&d]showing: distorted lung architecture, collapsed alveoli(A),extrusion of some cells into alveolar lumen (curved arrow),obvious increase in type 2 pneumocytes(p2) and alveolar macrophage (M),marked increase in thickness of interalveolar septum (arrow), wide spread dilated congested blood capillaries(BV) and type 1 pneumocytes (P1)is also observed.

(Toluidine blue × 1000, Scale bar = 10 µm)

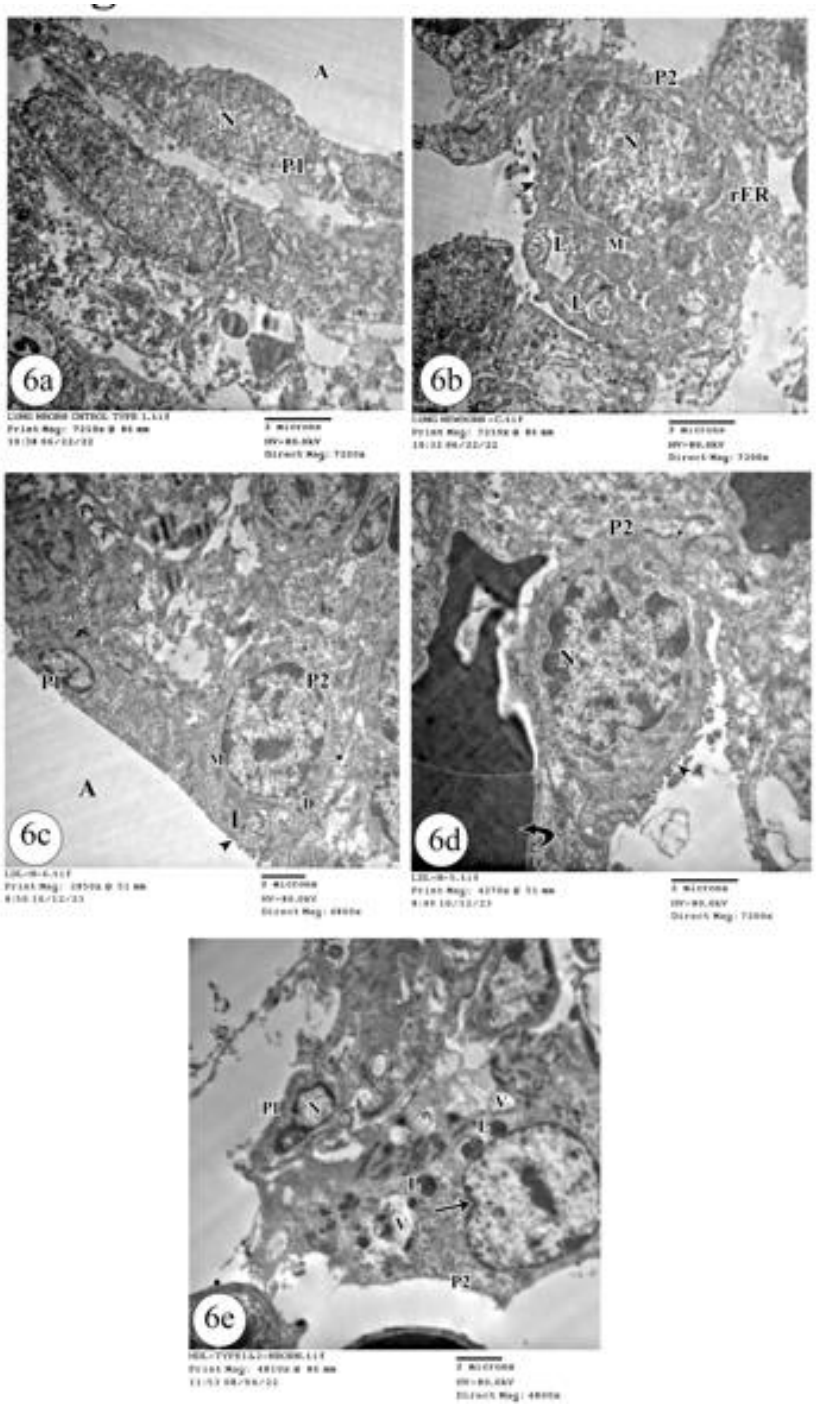

Fig.6: Electron micrographs of newborn lung from control (a, b), low dose (c, d) and high dose (e) groups. [6a] showing: the alveoli (A) and type 1 pneumocytes (P1) with its characteristic flattened euchromatic nucleus (N) and thin rim of cytoplasm.[6b] showing: type 2 pneumocytes (P2) with large round euchromatic nucleus(N) ,lamellar bodies (L) and mitochondria (M),Rough endoplasmic reticulum (R)and characteristic alveolar border (arrow head) are noticed.[6c]showing: alveoli (A),type 1 pneumocyte (P1) ,type 2 pneumocyte (P2)with round hyperchromatic nucleus (N),lamellar bodies (L),mitochondria (M),lipid droplets(D) and characteristic micro alveolar border (arrow head).[6d] showing :type 2 pneumocyte (P2) has heterochromatic nucleus(N) with clumped chromatin, and characteristic alveolar border(arrow head).extravasation of RBCS (curved arrow) is also noticed [6e] showing : type I pneumocyte (P1) exhibits shrunken nucleus (N) and type 2 pneumocyte (P2) exhibits indentation in nucleus (arrow),vacuoles in cytoplasm (V) ,multiple lipid droplets (L).
(TEM × 4800 In c, e TEM X 7200 in a, b, d Scale bar = 2 µm)

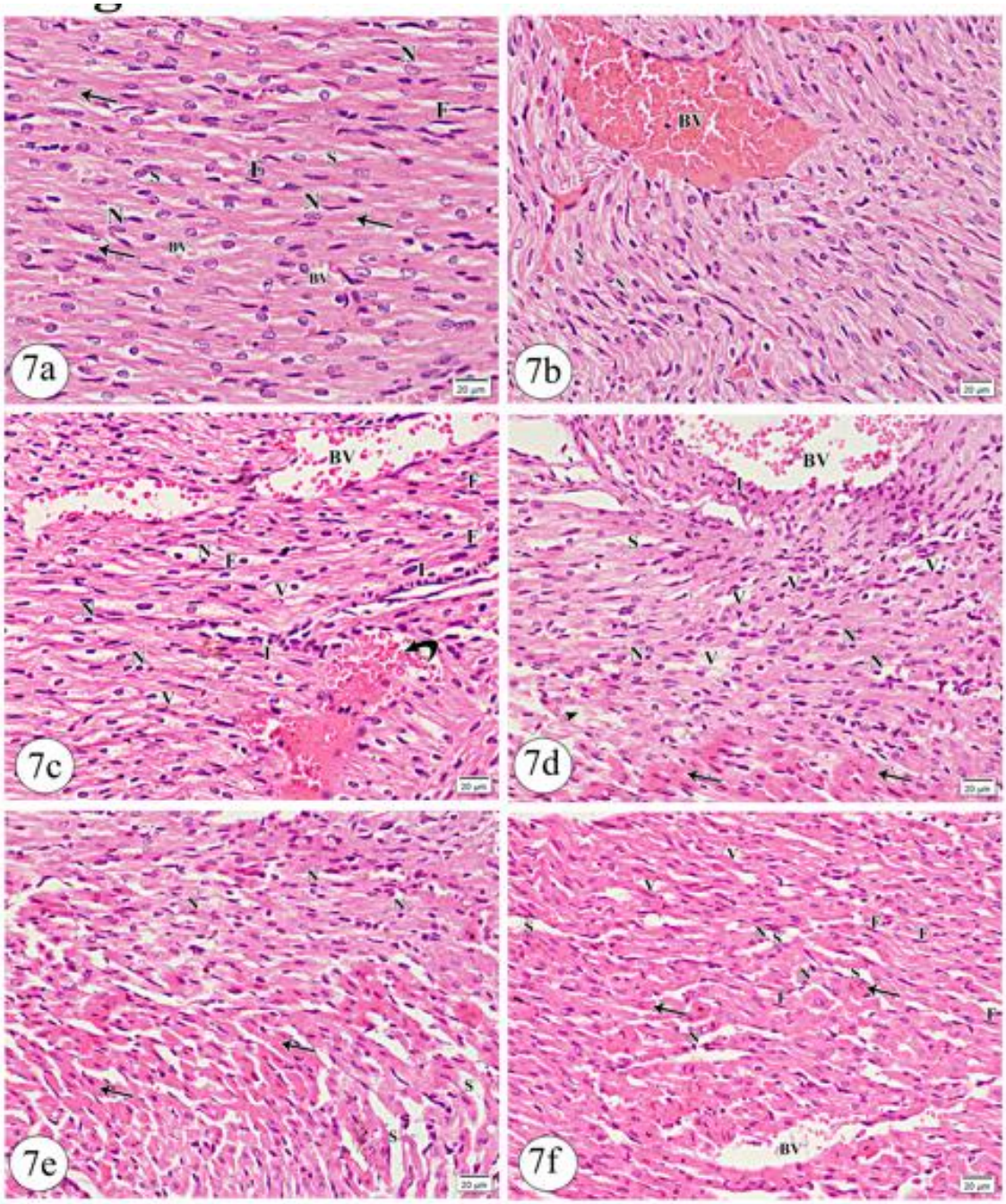

Fig.7 photomicrographs of longitudinal sections in ventricular wall of 21-day old albino rats of control(7a), low dose (7b, 7c) and high dose (7d, 7e, 7f) groups. [7a] showing: the typical branching and anastomosing cardiomyocytes with large oval central vesicular nucleus (N) and acidophilic sarcoplasm (arrow). In between the cardiomyocytes in connective tissue space the flattened fibroblast (F) and the blood capillaries (BV) are noticed. [7b,7c]showing: Dilated congested blood capillaries (BV),extravasation of blood cells between the cardiomyocytes(curved arrow) ,perivascular cellular infiltration(I),some nuclei appeared rounded and deeply stained (N),vacuoles in sarcoplasm (V) are also noticed.[7d,7e,7f]showing: the cardiomyocytes appeared disorganized with highly acidophilic sarcoplasm(arrow) ,some nuclei appeared rounded, deeply stained(N), area of lysis and degeneration (arrow head) are noticed. Dilated congested blood vessels (BV)and perivascular cellular infiltration (I), apparent increase in fibroblast (F) and wide space between the cardiomyocytes (S) are detected.
(H&E × 400, Scale bar = 20 µm)

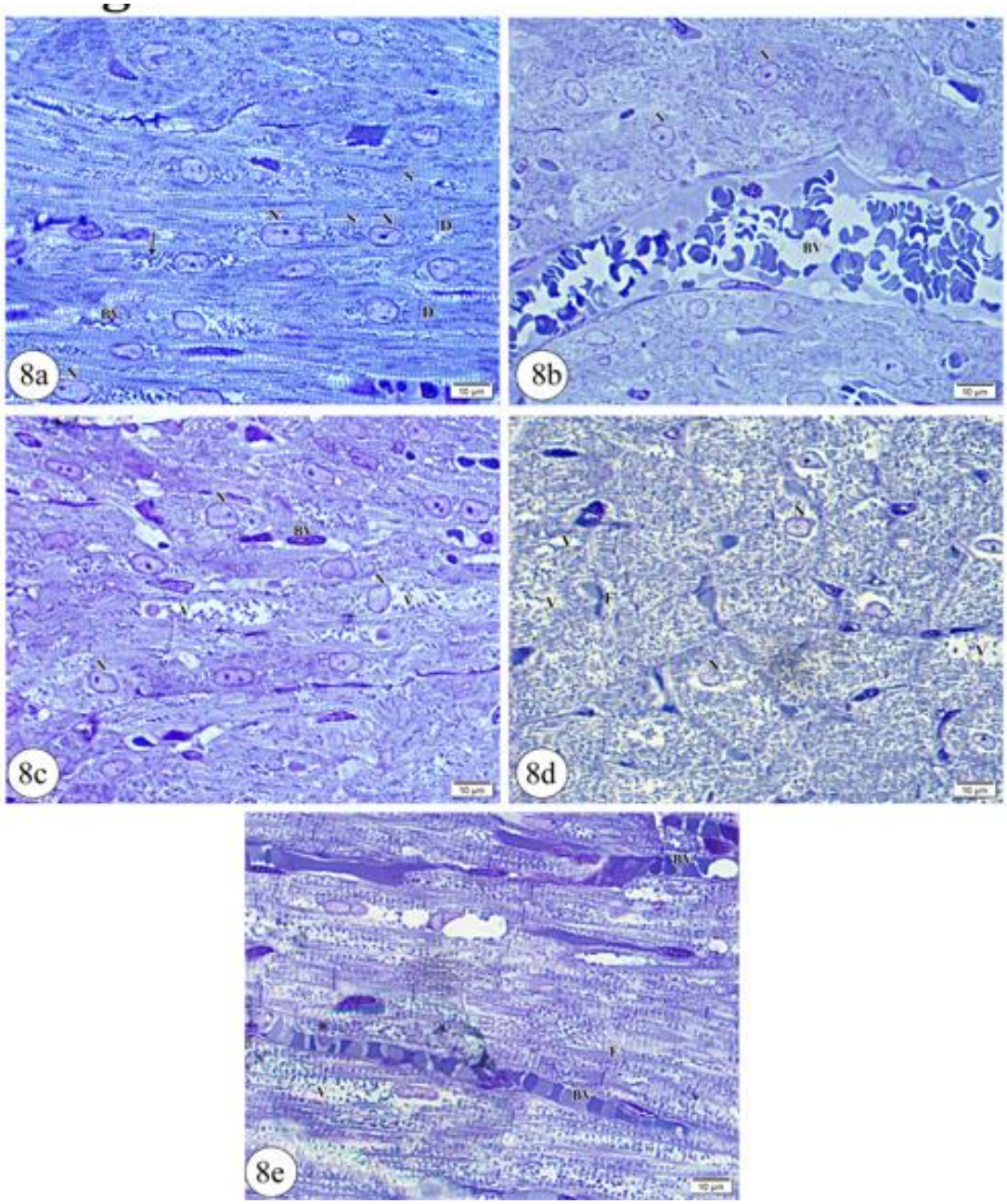

Fig.8 photomicrographs of semithin sections in 21day old albino rat of control[8a], low dose[8b ,8c] and high dose[8d, 8e] groups.[8a] showing: the characteristic striations of cardiomyocytes (S),central oval vesicular nucleus (N) ,normal sarcoplasm (arrow) and intercalated disc (D).blood vessels(BV) in connective tissue space are also detected.[8b,8c]: showing, most of nuclei lost their normal oval shape(N) ,vacuolated sarcoplasm (V) and dilated congested blood vessels (BV).More ever, The striations and intercalated disc not well demarcated.[8d,8e]:showing, marked thinning and degeneration of myofibers(F) ,most of nuclei appeared rounded and small(N) ,vacuolated cytoplasm(V) and markedly dilated congested blood capillaries(BV).

(Toluidine blue × 1000, Scale bar = 10 µm)

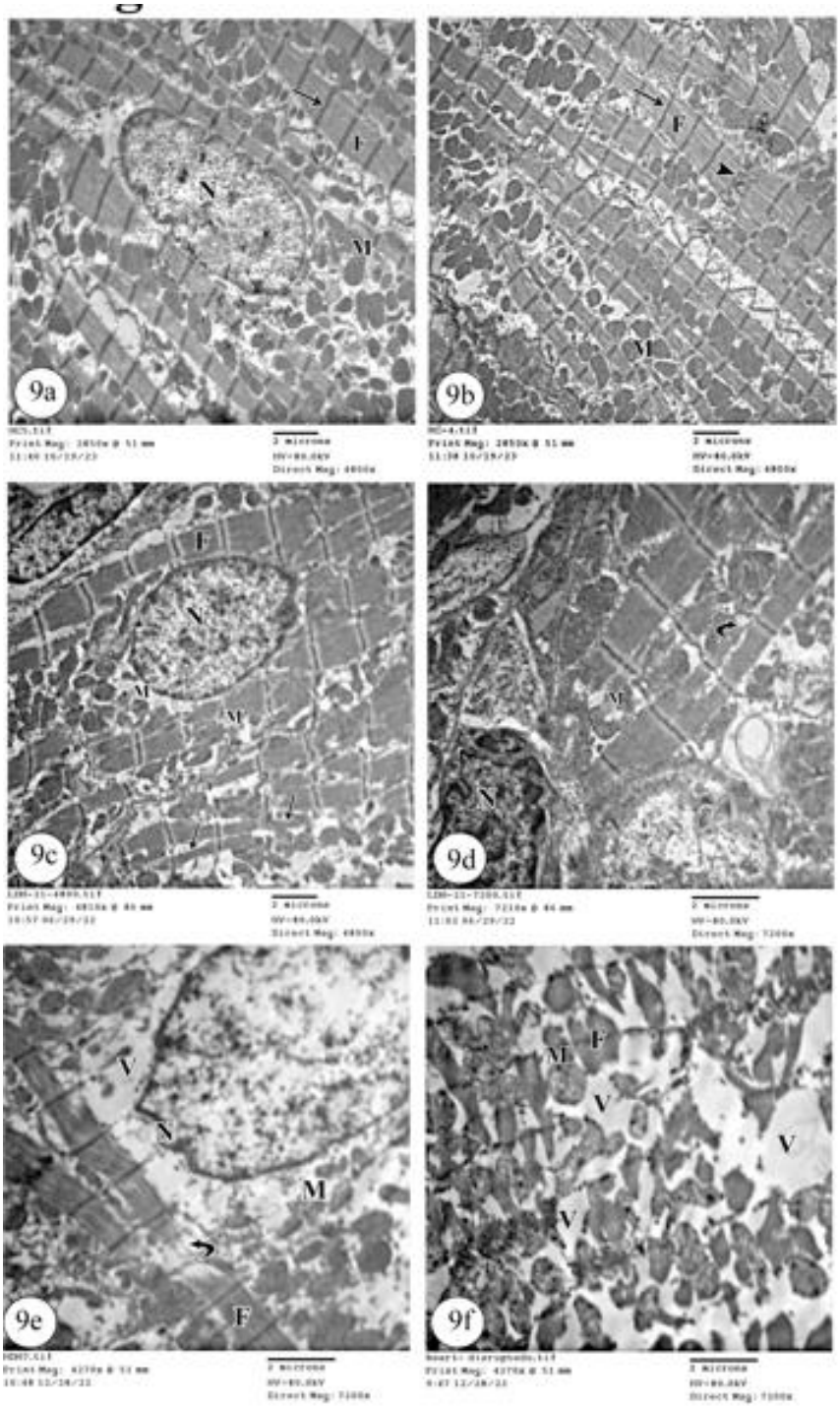

Fig.9 Electron micrographs of longitudinal sections in left ventricle of 21-day old albino rat of control (9a &9b), low dose (9c, 9d) high dose (9e& 9f) groups. [9a&9b]: showing, cardiomyocytes with their large oval euchromatic nucleus (N) and juxtanuclear abundant intact mitochondria(M). The myofibrils (F) with its characteristics striations (arrow) were regularly parrel arranged, intact intercalated disc (arrowhead) and abundant intact mitochondria(M) in between the myofibrils were also noticed. [9C&D] showing: preserved regularly arranged myofibrils(F) but thinning of some myofibrils is observed(arrow),abnormal shaped heterochromatic nucleus (N),destructed mitochondria(M) and degenerated area (curved arrow) in some myofibrils are also noticed.[9 e&f]:showing, complete loss of regular pattern of myofibril with area of degeneration and lysis (curved arrow),abnormally indented nucleus (N),massive destruction of mitochondria (M)and extensive vacuolization of cytoplasm(V).
(TEM × 4800 In a,b, TEM X 7200 in c, d,e and f Scale bar = 2 µm)

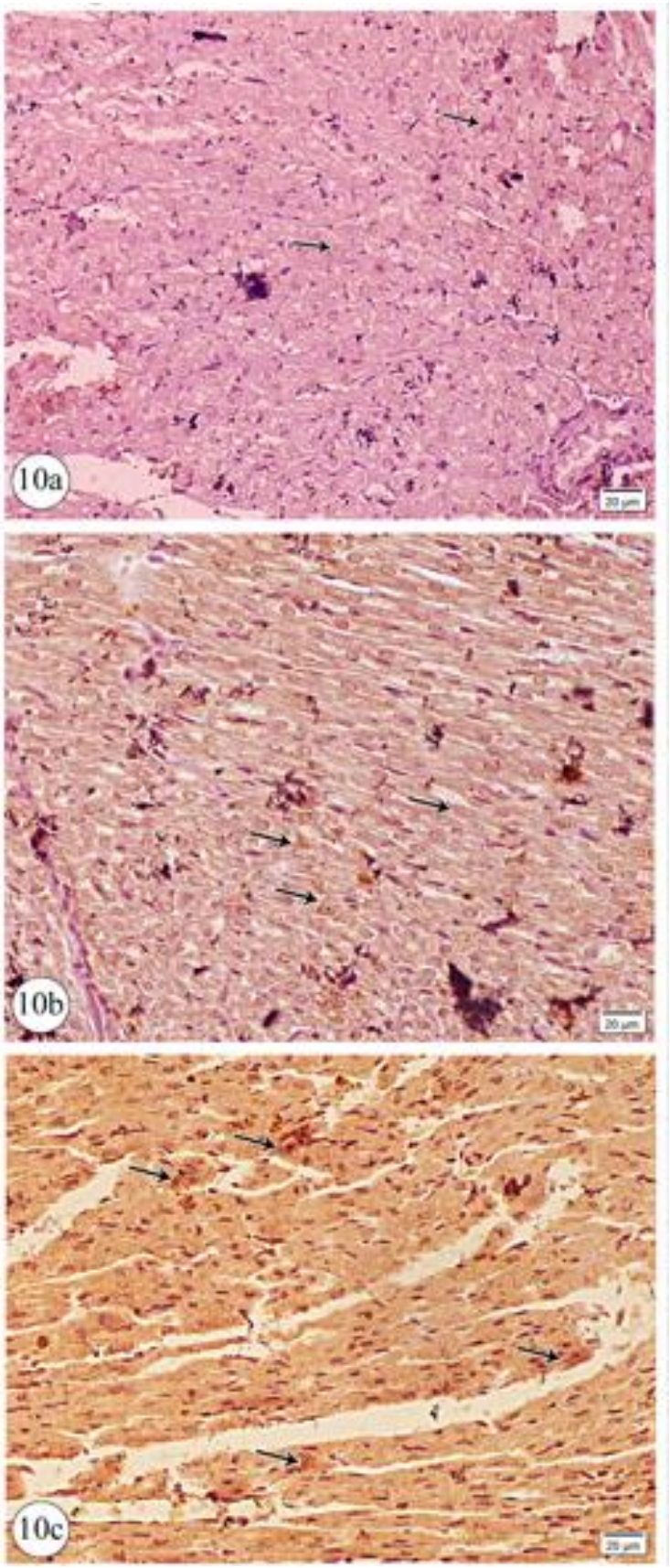

Fig.10 photomicrographs of INOS immunostaining of cardiac muscle in 21-day old rat of control(10a), low dose(10b) and high dose (10c) groups. [10a] showing minimal light brown positive INOS immunostaining of cytoplasm (arrow). [10b] showing moderate positive INOS immunostaining of cytoplasm(arrow). [10c] showing strong positive INOS immunostaining of cytoplasm (arrow).
(INOS immunohistochemical staining × 400, Scale bar = 20 µm)

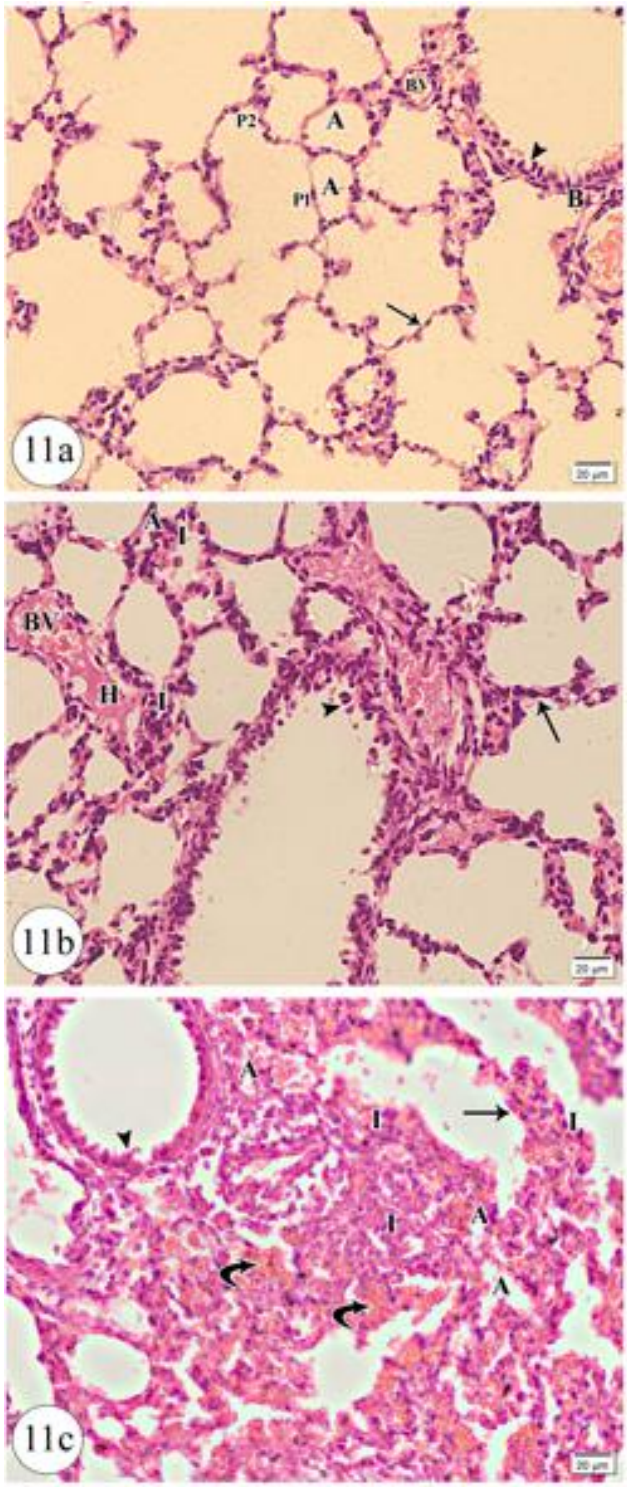

Fig.11 photomicrographs of longitudinal sections of lung 21-day old rat of control(11a), low dose(11b), and high dose(11c) groups. [11a]: showing, patent alveoli(A), thin interalveolar septum(arrow) lined by flattened type 1 pneumocytes(p1) and cuboidal type 2 pneumocytes (p2), bronchiole(B) lined by stratified bronchiolar epithelium (arrowhead) and blood vessels (BV) are observed. [11b]: showing, collapsed alveoli(A), apparent increase in thickness of interalveolar septum (arrow), cellular infiltrations(I), destroyed bronchial epithelium (Arrowhead) and congested blood vessels (BV)with deposition of hyaline material(H) in it. [11c] showing severe massive destruction of lung architecture, several alveoli are collapsed(A), massive cellular infiltration (I) and marked apparent thickening of interalveolar septum(arrow). Distorted bronchial epithelium (Arrowhead) and extensive extravasation of red blood cells (curved arrow) are apparent. **(H&E × 400, Scale bar = 20 µm).**

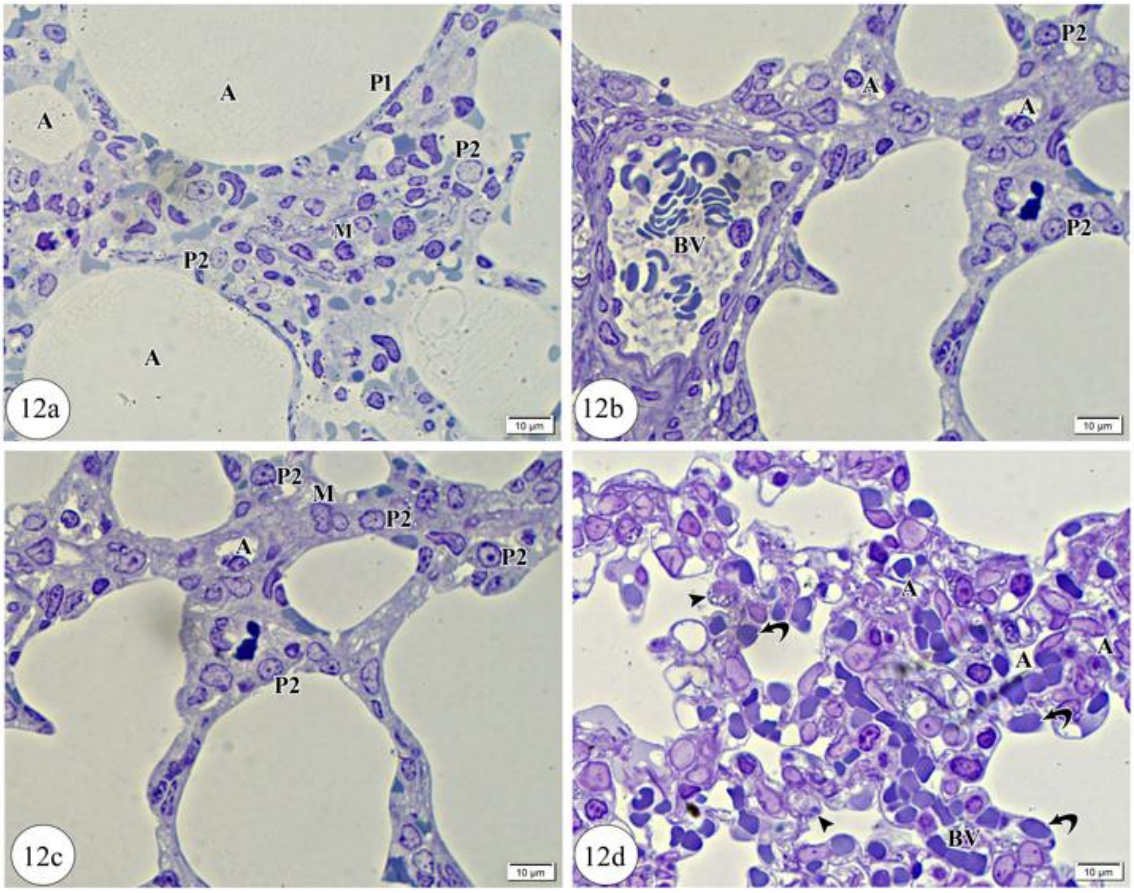

Fig.12 photomicrographs of semithin sections of lung in 21 days old albino rats from control (12a),low dose (12b&12 c) and high dose(12d) groups.[12a]: showing the patent alveolar lumen (A) lined with type 1 pneumocyte (P1) with its characteristic flattened appearance ,few number of type 2 pneumocytes (P2) with large rounded nucleus and macrophage (M) with its characteristic kidney shaped nucleus was noticed.[12b&c]:showing, collapsed alveoli (A) with extrusion of pneumocytes into the alveolar lumen ,dilated congested blood capillaries (BV)and apparent increase in number of type 2 pneumocytes (P2).[12d]:showing complete loss and distortion of normal lung architecture with extrusion of cells into the alveolar lumen (arrow head),several collapsed alveoli (A),dilated congested blood capillaries all over the lung (BV) and extravasation of red blood cells(curved arrow).

(Toluidine blue × 1000, Scale bar = 10 µm)

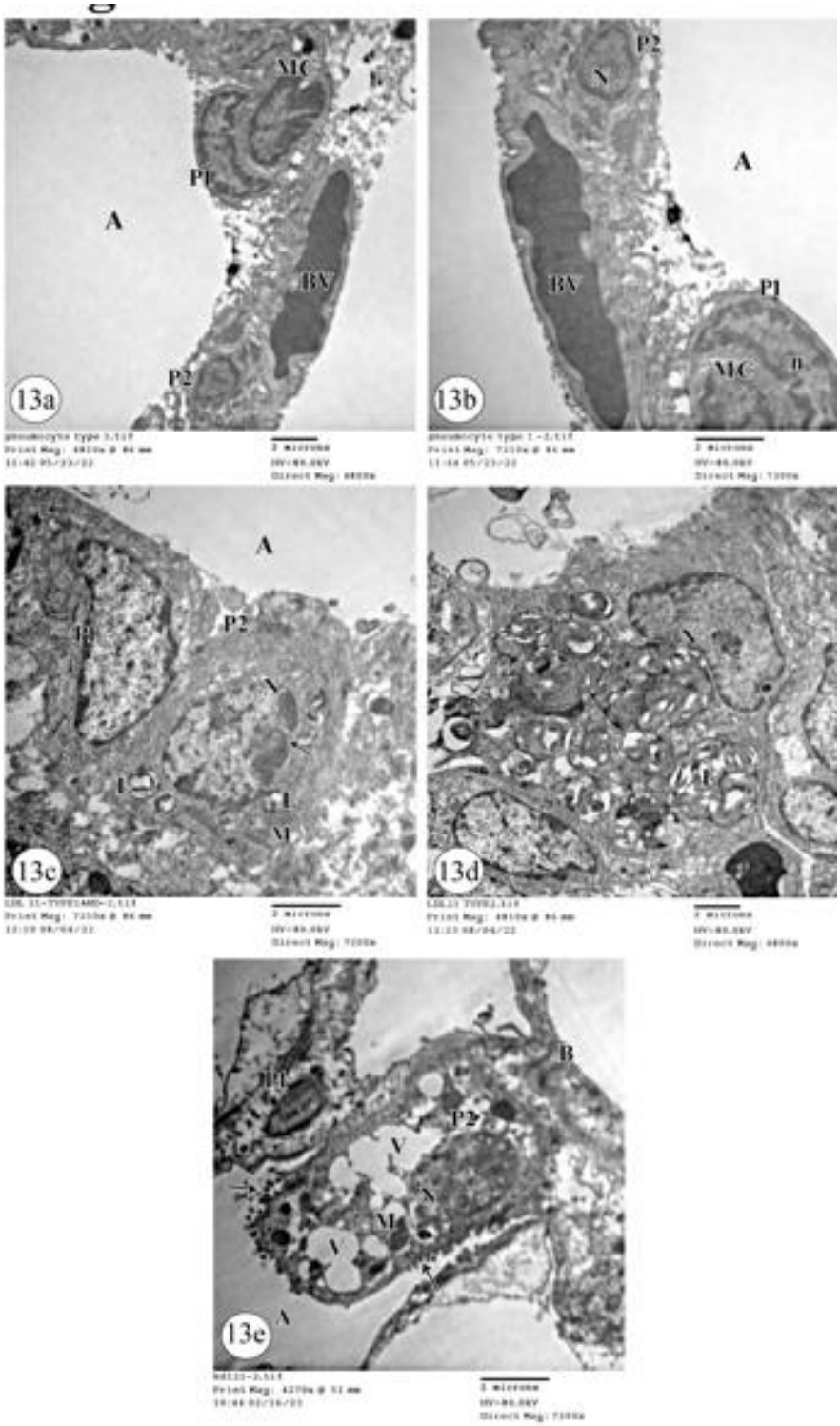

Fig.13 Electron micrographs of longitudinal sections of lung in 21 day old rat of control(13a &13b),low dose (13c&13 d),and high dose(13e) groups.[13 a, b]showing: alveoli (A), type 1 pneumocyte (P1) with flattened euchromatic nucleus(n), type 2 pneumocyte(P2) with large round euchromatic nucleus(N), alveolar macrophage(MC) with kidney shaped nucleus, and blood vessels(BV) are noticed. [13c,d]: showing, alveoli (A) with type 1 pneumocytes (p1),type 2 pneumocyte (p2) with heterochromatic(N) indented nucleus(arrow) and vacuolated lamellar bodies(L) ,ballooned mitochondria(M).[13e]:showing, alveoli (A),bronchiole(B), abnormal shrunken type 1 pneumocyte (p1) ,type 2 pneumocytes (p2) with shrunken heterochromatic indented nucleus(N) ,multiple vacuolated lamellar bodies(V), micro alveolar border(arrow) and ballooned swollen mitochondria (M).

(TEM × 4800 In a, c TEM X b, d, e7200 in Scale bar = 2 µm)

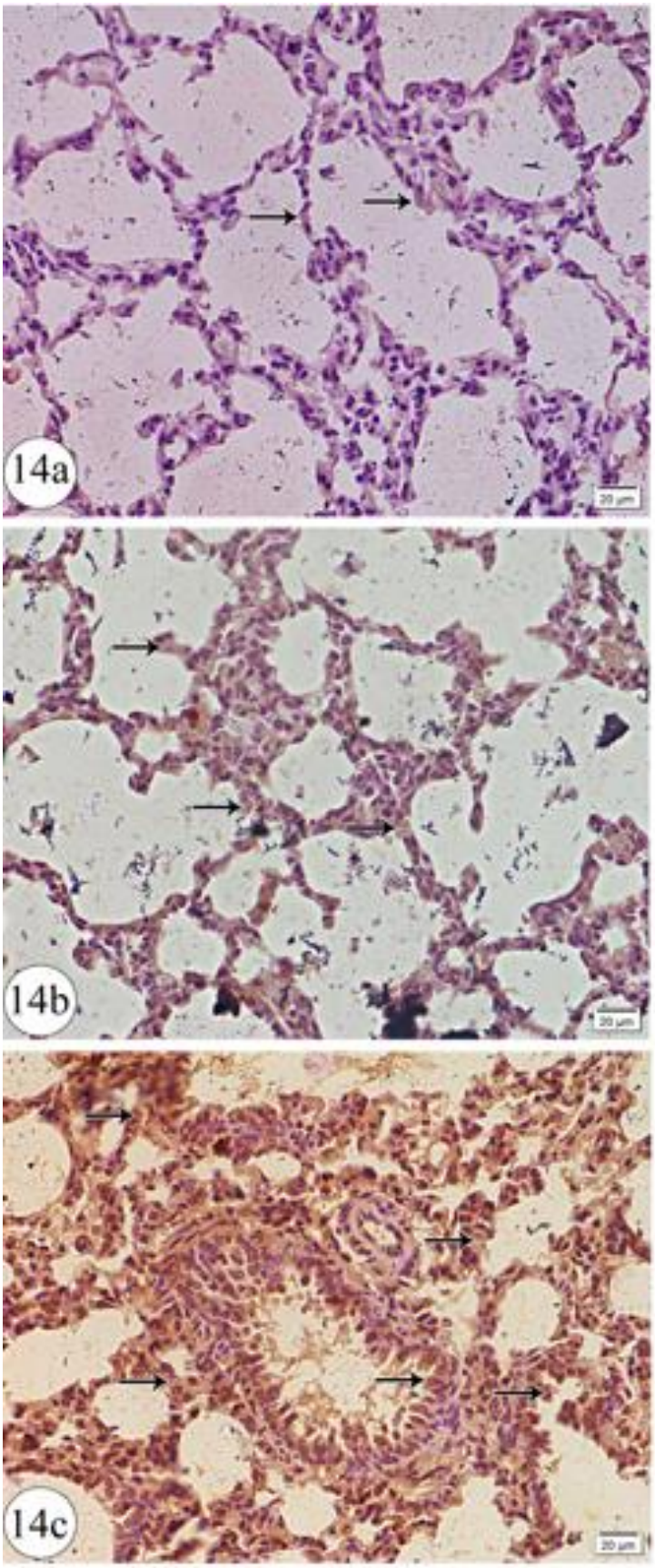

Fig.14 photomicrographs of INOS immunostaining of longitudinal sections of lung of 21-day old rat of control(14a), low dose(14b), and high dose(14c) groups. [14a]: showing, minimal positive immunoreaction(arrow). [14b]: showing moderate positive immune reaction (arrow). [14c]: showing strong positive immune reaction (arrow).
(INOS immunohistochemical staining × 400, Scale bar = 20 µm

2.4. Statistical and Morphometric Examination:

The statistical and morphometric analysis showed that the low-dose and high-dose treated groups revealed a noteworthy rise in the thickness of inter-alveolar septum as compared to the control group in newborns as well as 21 days old rats as illustrated in (Table 1) and (Fig. 15& 16).

Table 1: Mean thickness of inter-alveolar septum in newborn and in age 21 days in the all groups.

Group	Control Group (Mean±SD) N=21	Low dose Group (Mean±SD) N=21	High dose Group (Mean±SD) N=21	P-value
thickness of interalveolar septum in newborn	15.7114±2.8217	29.5261±5.9444	29.9100±4.5579	0.000
thickness of interalveolar septum in 21 days	13.2380±3.1298	18.9933±4.8451	23.6009±4.5447	0.000

- Data presented as mean±SD, test used multivariate ONEWAY ANOVA.
- P-value is significant P<0.05

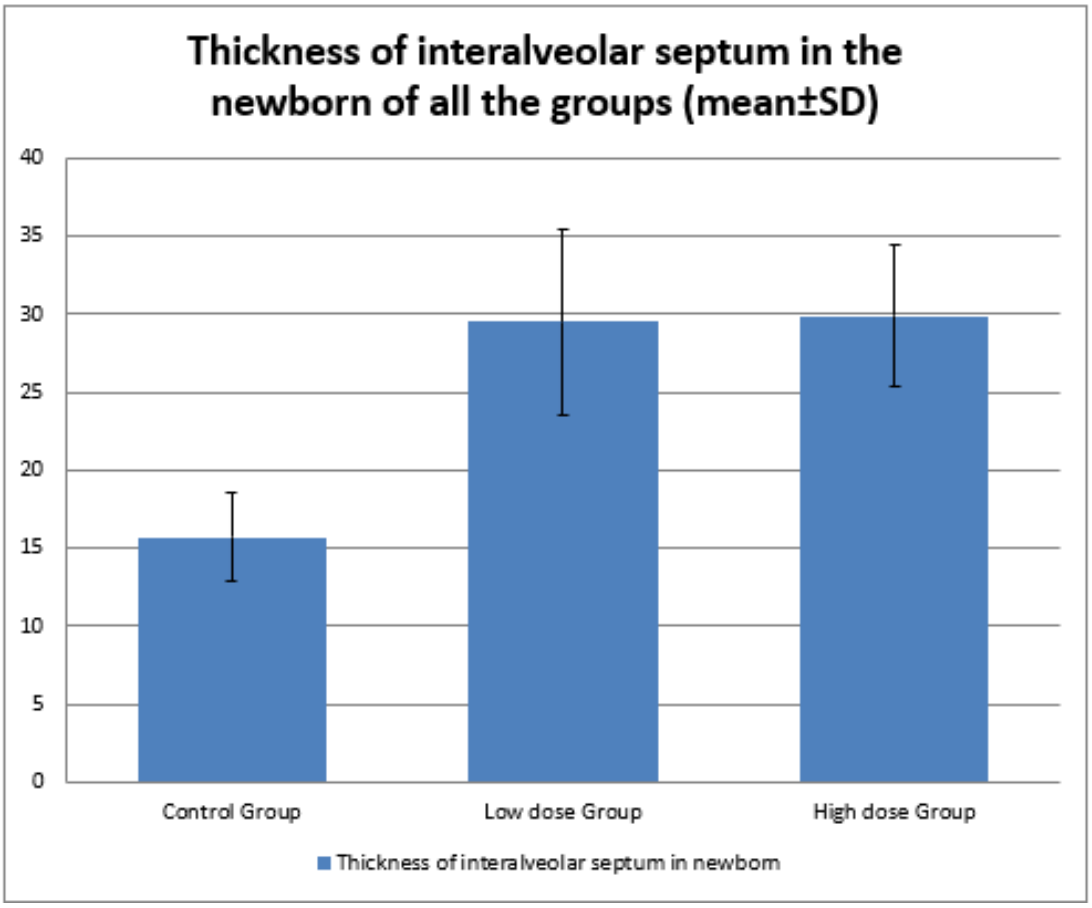

Fig. 15: thickness of inter-alveolar septum in the newborn of all the groups. Data presented as mean±SD

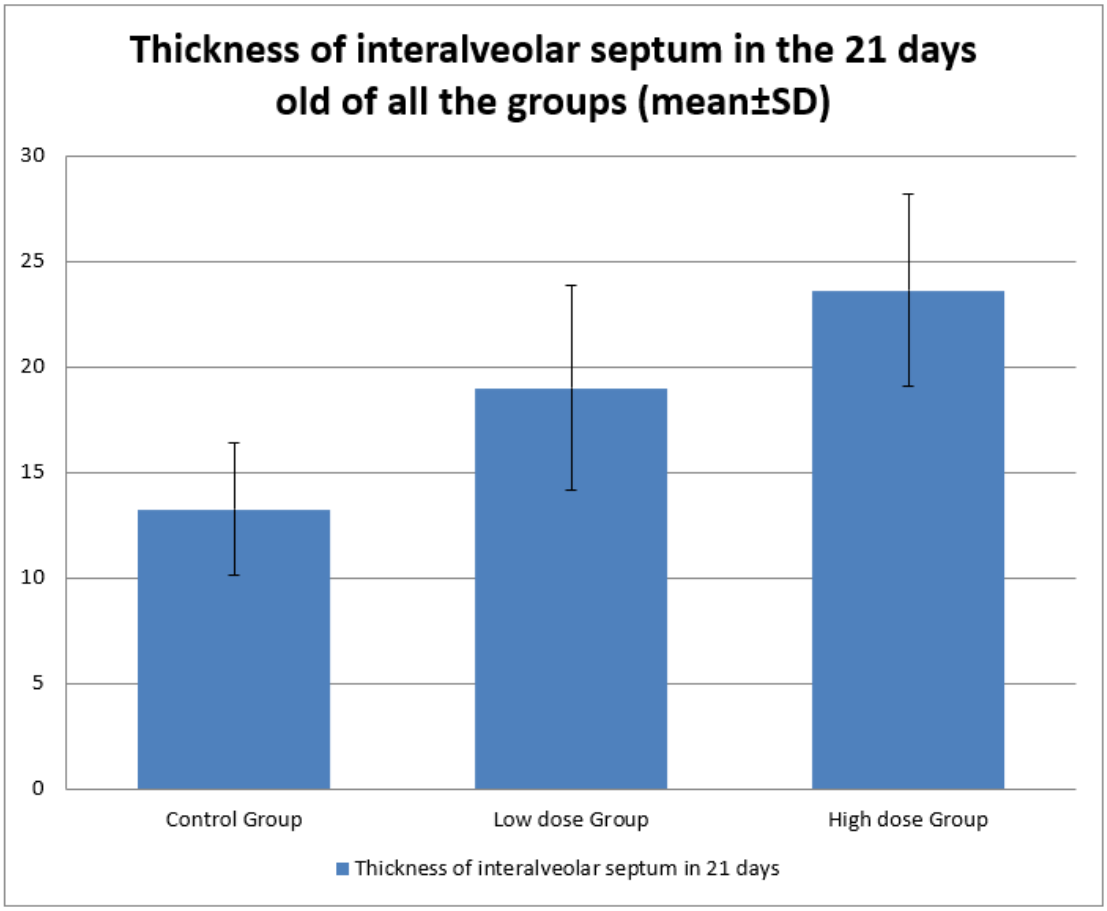

Fig. 16: thickness of inter-alveolar septum in the 21 days old of all groups. Data presented as mean±SD

DISCUSSION

In recent years, energy drinks, or ED, have gained significant attention as a health concern. Despite their purported safety and benefits, ED has been linked to fatal consequences (Kaur *et al.*, 2022). High energy drink consumption is linked to a rapid disturbance in the hemodynamic state as elevated glucose and nor-epinephrine levels, along with elevated heart rate, even in young healthy adults without any cardiovascular risk factors, elevated arterial blood pressure and palpitations exacerbate cardiovascular issues (Sanchis *et al.*, 2016). In addition to the dangerous cardiovascular complications reported above, consumption of ED negatively affects many systems of the human body: the nervous system; headache, discomfort, irritability, excitability, nervousness, insomnia, and GIT; malaise, dehydration, nausea, vomiting, abdominal pain, and xerostomia (Nowak *et al.*, 2018). Because albino rats and humans are similar in structure and function, albino rats were the preferred animals for this work. Moreover, the results of several studies conducted on albino rats were frequently comparable to those conducted on humans (Sengupta, 2013).

In the course of this experimental work, consumption of Red Bull in the peri-natal period with low dose and high dose revealed marked histological, immunohistochemical and morphometric changes in the heart and lung of newborn and twenty-one days old albino rats' offsprings. These changes were more obvious and more dangerous in the high-dose group. In hematoxylin and eosin-stained sections of the heart, there were disturbances of regular pattern arrangement of myofibrils, nuclei appeared degenerated, small and pyknotic, the sarcoplasm showed many vacuoles, became highly acidophilic and blood vessels appeared dilated and congested with perivascular cellular

infiltration moreover, the blood vessels ruptured in some areas with extravasation of red blood cells. In toluidine, blue-stained semithin sections marked thinning of myofibrils with loss of characteristic striation and intercalated disc not well demarcated with loss of oval shape in most of the nuclei. This came in accordance with Kaur *et al.*, 2022 who stated that the use of ED has been connected to potentially deadly circulatory system side effects such as cardiomyopathy, myocardial infarctions, atrial and ventricular arrhythmias, and sudden cardiac arrest. Large amounts of taurine, sugars, B vitamins, and caffeine are responsible for these effects, which also lengthen the QTc and raise blood pressure, heart rate, and cardiac contractility (Kaur *et al.*, 2022).

The most serious adverse effects of energy drinks on the heart are attributed to their caffeine content as Caffeine acts as an antagonist of adenosine as it acts on adenosine receptors A1, A2A, and A2B (Sawynok, 2011). Adenosine performs its action on the vascular receptors, leading to dilatation of the vascular beds. Caffeine inhibits the vasodilatory effect of adenosine by acting as an antagonist. Additionally, caffeine raises the plasma concentration of adenosine by blocking adenosine receptors. Catecholamine levels, peripheral vascular resistance, sympathetic tone, and renin secretion all rise as a result. This could clarify the process by which ED causes a sudden elevation in blood pressure and heart rate (Echeverri *et al.*, 2010).

Another explanation for how energy drinks can affect the heart is that vitamin B12 and folic acid (components of energy drinks) can decrease the level of homocysteine. The enzyme methionine synthase catalyzes the remethylation of homocysteine to methionine, which requires folate and vitamin B12 (Fratoni and Brandi, 2015). Therefore, homocysteine levels, a risk factor for cardiovascular diseases, are lowered by folate and vitamin B12 (Ma *et al.*, 2017).

Sugar in the form of high-fructose corn syrup, sucrose, or glucose is one of the ED ingredients (Bedi *et al.*, 2014). Consumption of sucrose and glucose together raised cardiac output and lowered peripheral resistance. Moreover, the heart rate is elevated by glucose, fructose, and sucrose (Grasser *et al.*, 2014). Research on rats indicates that sucrose elicits the sympathetic nervous system, resulting in an increase in renin secretion, heart rate, renal sodium retention, and vascular resistance, all of which contribute to hypertension (DiNicolantonio and Lucan, 2014). In the same manner, glucose increases cardiac output through two different mechanisms: vasodilation linked to insulin secretion and an increase in sympathetic activity first (Synowski et al., 2013).

Our results also came in line with Demirel et al., 2023 who stated that rats in the Red Bull group showed numerous inflammatory cellular infiltrations, damage to their cardiomyocytes and in certain areas of the heart walls, abnormalities in the vascular endothelium were found (Demirel *et al.*, 2023).

In this study, ultra-structural changes were detected in the heart after consumption of Red Bull, thinning and degeneration of myofibrils in some regions, vacuolated rarified cytoplasm, destructed mitochondria, and abnormal indentation in nuclei. This came in accordance with Munteanu *et al.*, 2018 who performed an experiment on alcohol and ED. In the hearts of rats given alcohol, they noticed symptoms of alcoholic cardiomyopathy, such as enlarged, damaged mitochondria with dilated crystals and an abnormal arrangement of myofibrils. Additionally, they observed abnormally large spaces between myofibrils and dilated crystals, and ballooned large mitochondria, in the rats that had ED, which was brought on by oxidative damage (Munteanu *et al.*, 2018).

These results also came in line with Mansy *et al.*, 2018, who compared

three groups of rats given three different doses of ED with the control group. They found that serum levels of antioxidant enzymes were lowered markedly in rats with medium and high ED doses (Mansy *et al.,* 2018).

In this study, peri-natal consumption of Red Bull in high and low doses revealed major changes in the lungs of newborn and twenty-one-day-old rats' offspring. In the hematoxylin and eosin-stained sections and in semithin sections there were disturbed lung architecture, collapsed alveoli, degenerated bronchiolar epithelium, marked increase in thickness of inter-alveolar septum, congested blood vessels and cellular infiltration in some regions and this came in accordance with Treml *et al.,* 2020 who stated that the effects of caffeinated energy drinks on the distribution of pulmonary ventilation and perfusion are poorly understood. He postulated that consuming Red Bull would modify the flow of blood through the lungs (Treml *et al.,* 2020).

A study was performed to find out if Red Bull has an impact on pulmonary blood flow or hypoxic pulmonary vasoconstriction (HPV). They observed after red pull consumption there was an increased shunt fraction during acute exposure to short-term hypoxia. In addition, they noticed elevated pvCO2 levels in hypoxia soon after consuming Red Bull. The possibility of a shunt-related decrease in pulmonary CO2 removal can be ruled out because arterial gas exchange seemed to be unaffected (Treml *et al.,* 2020).

ED consumption augments physiologic responses to hypoxia and cardiovascular adverse effects in high altitudes. Reduced inspired PaO2 at high altitudes causes hypoxia-mediated contraction of the pulmonary smooth muscle blood vessels without a decrease in gas exchange, and hypoxic pulmonary vasoconstriction, or HPV, takes place. Caffeinated energy drinks have the potential to worsen hypoxemia if they disrupt ventilation or perfusion. Furthermore, consuming Red Bull may significantly increase the risk of hypoxia-induced tachycardia (Smirmaul *et al.,* 2016) & (Stadheim *et al.,* 2015).

Numerous human case reports and studies about patients who used ED and other high-sugar, high-caffeine beverages and ended up in hospitals with lung issues like asthma attacks and bronchospasm can be found in the literature. Varraso *et al.,* 2009 showed that a diet heavy in carbohydrates caused an asthma attack (Varraso et al., 2009). Wood *et al.,* 2011 reported that the quick switch to a diet high in carbohydrates had a negative impact on airway inflammation (Wood *et al.,* 2011).

In this experiment, several ultra-structural changes were noticed after consumption of Red Bull in low and high-dose groups as, indentation of nuclei, vacuolated lamellar bodies and ballooned mitochondria, heterochromatic shrunken nuclei and dilated rough endoplasmic reticulum and this came in agreement with Demirel *et al.,* 2023 who stated that, analysis of animal's blood gas, The difference between ED and the other groups was statistically significant (P=0.05). While the study groups' median PaCO2 and PaO2 were comparable, the ED group's values were lower (Demirel *et al.,* 2023).

Conclusion

In conclusion consumption of Red Bull during the peri-natal period induced marked histological, ultra-structural, immunohistochemical and morphological damage in the heart and lungs of the offspring, especially high dose consumption. So, it is not preferred to have Red Bull during pregnancy and lactation and Further studies are needed regarding biochemical aspects.

Declarations:

Ethical Consideration: Ethical approval from the Ethics Committee of the Faculty of Medicine, Assiut University, Egypt was obtained with local approval number (IRB: 17300931) in accordance with the international guidelines of the Animal Care and Use Committee guidelines.

Conflict of Interest: The authors declare that they have no conflict of interest.

Author contribution: Each author took part in the design of the study, contributed to data collection, and participated in writing the manuscript. The manuscript is neither being published nor being considered for publication elsewhere until a decision is reached by this journal.

Data availability statement: Data related to this research can be obtained from the author based on appropriate request.

Funding Information: The author received no funding for this work.

Acknowledgment: The author is grateful to all laboratory technicians for their efforts and time.

REFERENCES

Adjene J., Emojevwe V., Idiapho D. (2014). Effects of long-term consumption of energy drinks on the body and brain weights of adult Wistar rats. *Journal of Experimental and Clinical Anatomy,* 13(1):17-20. DOI: 10. 4103/ 1596-2393.142925.

Al Drees A, Salah Khalil M, Soliman M (2017). Histological and Immunohistochemical Basis of the Effect of Aminoguanidine on Renal Changes Associated with Hemorrhagic Shock in a Rat Model. *Acta Histochemica Cytochemica,* Feb 28;50(1):11-19. doi: 10.1267/ahc.16025. Epub 2017 Feb 22. PMID: 28386146; PMCID: PMC 5374099.

Al-Basher GI, Aljabal H, Almeer RS, Allam AA, Mahmoud AM. (2018). Perinatal exposure to energy drinks induces oxidative damage in the liver, kidney and brain, and behavioral alterations in mice offspring. *Biomedicine & Pharmacotherapy,*102: 798-811.doi: 10.1016/j.biopha.2018. 03.139. Epub 2018 Apr 5. PMID: 29605768.

Bancroft, JD & Layton C (2019). The hematoxylin and eosin in: Suvarna SK, Layton C and Bancroft JD, editors Bancroft's Theory and Practice of Histological Techniques, 8th Edition, Chapter 10, Elsevier Limited, 126-138.

Bedi N, Dewan P, Gupta P (2014). Energy drinks: potions of illusion. *Indian Pediatrics,* ;51(7): 529-33. doi: 10.1007/s 13312-014-0441-9. PMID: 25031128.

Connelly LM (2021). Introduction to analysis of variance (ANOVA). *Medsurg Nursing,* 30:158–218.

Curran CP, Marczinski CA (2017). Taurine, caffeine, and energy drinks: Reviewing the risks to the adolescent brain. *Birth Defects Research,* 1;109(20): 1640-1648. doi: 10.1002/bdr2. 1177. PMID: 29251842; PMCID: PMC5737830.

Demirel A, Başgöze S, Çakıllı K, Aydın Ü, Erkanlı Şentürk G, Örnek Diker V, Ertürk M (2023). Histopathological Changes in the Myocardium Caused by Energy Drinks and Alcohol in the Mid-term and Their Effects on Skeletal Muscle Following Ischemia-reperfusion in a Rat Model. *Anatolian Journal of Cardiology,*.27(1):12- 18.doi: 10.14744/AnatolJCardiol.2022. 2003.PMID: 36680442; PMCID: PMC9893703.

DiNicolantonio JJ, Lucan SC (2014). The wrong white crystals: not salt but sugar as aetiological in hypertension and cardiometabolic disease. *Open Heart*; 1: e000167. http://dx. doi.org/10.1136/openhrt-2014-000167.

Echeverri D, Montes FR, Cabrera M, Galán A, Prieto A (2010). Caffeine's Vascular Mechanisms of Action. International journal of vascular medicine; 2010:834060. doi: 10.1155/2010/834060. Epub 2010 Aug 25. Erratum in: *International Journal* of *Vascular Medicine,*2019

Nov 20; 2019:7480780. PMID: 21188209; PMCID: PMC 3003984.

Fratoni V, Brandi ML (2015). B vitamins, homocysteine and bone health. *Nutrients,* 30;7(4): 2176-92. doi: 10.3390/nu 7042176. PMID: 25830943; PMCID: PMC4425139.

•Geith IM (2017). Clinical pathology of caffeinated and non-caffeinated energy drinks. *Life Science Journal;*14(9): 21-36. DOI:10. 7537/marslsj140917.03.

Grasser EK, Dulloo A, Montani JP (2014). Cardiovascular responses to the ingestion of sugary drinks using a randomized cross-over study design: Does glucose attenuate the blood pressure-elevating effect of fructose? *British Journal of Nutrition,* 28;112(2): 183-92. doi: 10.1017/ S0007114514000622. Epub 2014 Apr 29. PMID: 24780643.

Grasser EK, Dulloo AG, Montani JP (2014). Cardiovascular and cerebrovascular effects in response to red bull consumption combined with mental stress. *American Journal of Cardiololgy,*15;115(2): 183-9.doi: 10.1016 /j. amjcard. 2014. 10.017. Epub 2014 Oct 29. PMID: 25465941.

Higgins JP, Tuttle TD, Higgin CL (2010). Energy beverages: contents and safety. *Mayo Clinic Proceedings;* 85: 10331041. DOI:10.4065 /mcp. 2010.0381.

Kaur A, Yousuf H, Ramgobin-Marshall D, Jain R, Jain R (2022). Energy drink consumption: a rising public health issue. *Reviews in Cardiovascular Medicine,* 23 (3):83. doi: 10.31083/j. rcm 2303083. PMID: 35345250.

Latifa Khayyat, Amina Essawy, Jehan Sorour and Maisaa Al Rawi (2014). Impact of Some Energy Drinks on the Structure and Function of the Kidney in Wistar Albino Rats. *Life Science Journal;* 11(10): 1131-1138]. (ISSN:1097-8135). www.lifesciencesite.com.170D OI:10.7537/ marslsj111014.170.

Ma Y, Peng D, Liu C, Huang C, Luo J (2017). Serum high concentrations of homocysteine and low levels of folic acid and vitamin B12 are significantly correlated with the categories of coronary artery diseases..*BMC Cardiovascular Disordor,* 21;17(1):37. doi: 10.1186/s 12872-017-0475-8. PMID: 28109191; PMCID: PMC 5251223.

Mansy W, Alogaiel DM, Hanafi M, Zakaria E (2018). Effects of chronic consumption of energy drinks on liver and kidney of experimental rats.*Tropical Journal of Pharmaceutical Resarch;*16(12):2849-2856.doi. org/10.4314/tjpr. v16i12.8.

•Munteanu C, Rosioru C, Tarba C, Lang C (2018). Long-term consumption of energy drinks induces biochemical and ultrastructural alterations in the heart muscle. *Anatolian Journal Cardiology,* May;19(5):326-323. doi:10.14744/AnatolJ Cardiol. 2018.90094. PMID: 29724975; PMCID: PMC 6280269.

Nowak D, Gośliński M, Nowatkowska K (2018). The Effect of Acute Consumption of Energy Drinks on Blood Pressure, Heart Rate and Blood Glucose in the Group of Young Adults. *International Journal of Environmental Research and Public Health,* 19;15(3):544. doi: 10.3390/ ijerph 15030544. PMID: 29562659; PMCID: PMC 5877089.

Olaleru F, Odeigah P (2015). Effects of energy drink on sperm morphology, hematological

parameters, and behavior of adult male mice. *Annual Research & Review in Biology*, 2015;6(5):288-296. DOI: 10. 9734/ARRB/2015/13573.

Sanchis-Gomar F, Leischik R, Lippi G (2016). Energy drinks: Increasing evidence of negative cardiovascular effects. *International Journal of Cardiology*, 1; 206:153. doi: 10. 1016/j.ijcard.2016.01.107.Epub 2016 Jan 8. PMID: 26797159.

Sawynok J (2010). Caffeine and pain. *Journal of the International association for the study of pain*, Apr;152(4):726-729. doi: 10. 1016/j.pain.2010.10.011.

Sengupta P (2013). The Laboratory Rat: Relating Its Age with Human's. *International Journal of Preventive Medicine*, Jun;4(6): 624-30. PMID: 23930179; PMCID: PMC3733029

Smirmaul BP, de Moraes AC, Angius L, Marcora SM (2017). Effects of caffeine on neuromuscular fatigue and performance during high intensity cycling exercise in moderate hypoxia. *European Journal of Applied Physiology*, Jan;117(1):27-38. doi: 10.1007/ s00421-016-3496-6.

Stadheim HK, Nossum EM, Olsen R, Spencer M, Jensen J (2015). Caffeine improves performance in double poling during acute exposure to 2,000-m altitude. *Journal of Applied Physiology*, Dec 15;119(12):1501-9. doi: 10. 1152/japplphysiol.00509.2015.

Synowski SJ, Kop WJ, Warwick ZS, Waldstein SR (2013). Effects of glucose ingestion on autonomic and cardiovascular measures during rest and mental challenge. *Journal of Psychosomatic Resarch*, Feb;74(2):149-54. doi: 10.1016/ j.jpsychores.2012.10.008.

Treml B, Schöpf E, Geiger R, Niederwanger C, Löckinger A, Kleinsasser A, Bachler M (2020). Red Bull Increases Heart Rate at Near Sea Level and Pulmonary Shunt Fraction at High Altitude in a Porcine Model. *Nutrients*, Jun 10;12(6):1738. doi: 10.3390/ nu12061738.

Uwaifo GI (2019). Beware Energy Drinks: A Case of a Toxic Triad Syndrome in a Diabetic Patient with Nonalcoholic Fatty Liver Disease. *American Journal of Medical Science*, Oct;358(4): 304-311.doi:10.1016/ j.amjms. 2019.07.015. Epub 2019 Aug 2. PMID: 31543103.

Varraso R, Kauffmann F, Leynaert B, Le Moual N, Boutron-Ruault MC, Clavel- Chapelon F, Romieu I (2009). Dietary patterns, and asthma in the E3N study. *European Respiratory Journal*, Jan;33(1):33-41. doi:10.1183/ 09031936.00130807. Epub 2008 Oct 1. PMID: 18829673; PMCID: PMC4761377.

Vercammen KA, Koma JW, Bleich SN (2019). Trends in Energy Drink Consumption Among U.S. Adolescents and Adults, 2003-2016. *American Journal of Preventive Medicine*, Jun; 56(6):827-833. doi: 10.1016/j. amepre.2018.12.007. Epub 2019 Apr 18. PMID: 31005465.

Wee JH, Min C, Park MW, Park IS, Park B, Choi HG (2021). Energy-drink consumption is associated with asthma, allergic rhinitis, and atopic dermatitis in Korean adolescents. *European Journal of Clinical Nutrition*, Jul; 75 (7):1077-1087. doi: 10.1038/s 41430-020-00812-2. Epub 2020 Nov 30. PMID: 33257845.

Wood LG, Garg ML, Gibson PG (2011). A high-fat challenge increases airway inflammation and impairs bronchodilator recovery in asthma. Journal of Allergy and *Clinical Immunology*, May;127(5):1133-40. doi: 10.1016/j.jaci. 2011.01.036.

Epub 2011 Mar 5. PMID: 21377715.

Woods, A. E. and Stirling, J. W. (2019). Transmission electron microscopy. In: Suvarna SK, Layton C, Bancroft JD, editors. Theory and Practical Histological Techniques. 8th edition, Chapter 21, Churchill.

ARABIC SUMMARY

هل التعرض في الفترة المحيطة بالولادة لمشروب الطاقه (السحب الأحمر) يؤدي إلى تلف القلب والرئة في نسل الجرزان: دراسة نسيجية ودقيقه التركيب ومناعيه كيميائية

هاله محمد حسانين محمد و سالي سيد انور

قسم التشريح الادمي وعلم الاجنه - كليه الطب -جامعه اسيوط- مصر

مقدمة: يتم استخدام مشروبات الطاقة في جميع أنحاء العالم. إن مكونات مشروبات الطاقه لها تأثيرات مرغوبة مثل زيادة الطاقة ولكنها تنتج تأثيرات غير مرغوب فيها على الصحة.

الهدف من الدراسه: تقييم آثار استهلاك الريد بول أثناء الحمل على بنية القلب والرئة.

المنهجية: أجريت هذه الدراسة على 30 فأراً أنثى بالغة حامل مقسمة إلى ثلاث مجموعات (10 في كل مجموعة). المجموعة الضابطة، المجموعة المعالجة بجرعة منخفضة من ريد بول (تلقت ريد بول 2.5 مل/كجم من وزن الجسم عن طريق الفم من اليوم الأول للحمل حتى اليوم الحادي والعشرين بعد الولادة، والمجموعة المعالجة بجرعة عالية من ريد بول (تلقت ريد بول 5 مل/كجم من وزن الجسم عن طريق الفم عن طريق الفم) من بداية الحمل حتى اليوم الحادي والعشرين بعد الولادة). يتم استخراج القلب والرئة عند حديث الولاده وعمر اليوم الواحد والعشرين.

النتائج: أدى استهلاك الريد بول إلى حدوث تغيرات مدمرة في القلب مثل فقدان الترتيب المنتظم لليفات العضلية وتمدد الأوعية الدموية المحتقنة وارتشاح الخلايا المحيطة بالأوعية الدموية ومناطق التنكس والتحلل. في الرئة، كان هناك تشوه في بنية الرئة، وزيادة في سمك الحاجز بين السنخية، وشذوذ في الخلايا الرئوية من النوع 1 و 2.

الخلاصة: إن تناول الريد بول في فترة ما حول الولادة، وخاصة بجرعات عالية، له آثار مدمرة على القلب والرئتين.